Neuroadaptive Output Feedback Control for Automated Anesthesia With Noisy EEG Measurements

Wassim M. Haddad, *Fellow, IEEE*, Kostyantyn Y. Volyanskyy, *Student Member, IEEE*, James M. Bailey, and Jeong Joon Im, *Student Member, IEEE*

***Abstract*—Critical care patients, whether undergoing surgery or recovering in intensive care units, require drug administration to regulate physiological variables such as blood pressure, cardiac output, heart rate, and degree of consciousness. The rate of infusion of each administered drug is critical, requiring constant monitoring and frequent adjustments. Nonnegative and compartmental models provide a broad framework for biological and physiological systems, including clinical pharmacology, and are well suited for developing models for closed-loop control of drug administration. In this paper, we develop a neuroadaptive output feedback control framework for nonlinear uncertain nonnegative and compartmental systems with nonnegative control inputs and noisy measurements. The proposed framework is Lyapunov-based and guarantees ultimate boundedness of the error signals. In addition, the neuroadaptive controller guarantees that the physical system states remain in the nonnegative orthant of the state space. Finally, the proposed approach is used to control the infusion of the anesthetic drug propofol for maintaining a desired constant level of depth of anesthesia for surgery in the face of noisy electroencephalographic (EEG) measurements. Clinical trials demonstrate excellent regulation of unconsciousness allowing for a safe and effective administration of the anesthetic agent propofol.**

***Index Terms*—Adaptive control, automated anesthesia, bispectral index, dynamic output feedback, electroencephalography, measurement noise, neural networks, nonnegative control, nonnegative systems, surgery.**

I. Introduction

THE DOSING of most drugs is a process of empirical administration of a low dose with observation of the biological effect and subsequent adjustment of the dose in the hopes of achieving the desired effect. This is true of anesthetic drugs, just as it is of chronically administered medications (for example, anti-hypertensive agents). In the acute environment of the operating room and intensive care unit (ICU), this can result in inefficient, and possibly even dangerous, titration of drug to the desired effect. There has been a long interest in use of the electroencephalograph (EEG) as an objective, quantitative measure of consciousness that could be used as a performance variable for closed-loop control of anesthesia [1]. Ever since the pioneering work of Bickford [2], it has been known that the EEG changes with the induction of anesthesia. Processed electroencephalogram algorithms have been extensively investigated as monitors of the level of consciousness in patients requiring surgical anesthesia [2]–[6]. However, the EEG is a complex of multiple time series and in earlier work it was difficult to identify one single aspect of the EEG signal that correlated with the clinical signs of anesthesia.

Subsequent to this early research there has been substantial progress in the development of processed EEG monitors that analyze the raw data to extract a single measure of the depth of anesthesia. The best known of these monitors is the bispectral or BIS monitor, which calculates a single composite EEG measure that is well correlated with the depth of anesthesia [1], [7], [8]. The BIS signal ranges from 0 (no cerebral electrical activity) to 100 (the normal awake state). Available evidence indicates that a BIS signal less than 55 is associated with lack of consciousness. While BIS monitoring has proven useful in the operating room environment, there have been inconsistencies reported and attempts to extend BIS monitoring for the evaluation of sedation outside of the operating room have been unsuccessful [9]. One of the key reasons for this is due to the fact that the signal-averaging algorithm within the BIS monitor ignores signal noise, and when there is excessive noise, the BIS monitor does not generate a signal.

It is widely appreciated that BIS monitoring, or for that matter, any EEG monitoring, can be fraught with error because of the potential for outside interference to produce an unfavorable signal-to-noise ratio yielding spurious results. Nonphysiologic artifactual signals may be generated from sources external to the patient that include lights, electric cautery devices, ventilators, pacemakers, patient warming systems, and electrical noise related to the many different kinds of monitors normally found in an operating room or ICU. Physiologic movements such as eye movements, myogenic activity, perspiration, and ventilation can produce artifactual increases in the BIS score. In particular, it is apparent that electromyographic (EMG) activity can spuriously increase the BIS score [10]. The co-administration of neuromuscular blockade eliminates artifacts from muscle movement, which

Manuscript received October 15, 2009; revised January 27, 2010. Manuscript received in final form February 03, 2010. First published March 11, 2010; current version published February 23, 2011. Recommended by Associate Editor N. Hovakimyan. This work was supported in part by the U.S. Army Medical Research and Material Command under Grant 08108002.

W. M. Haddad and K. Y. Volyanskyy are with the School of Aerospace Engineering, Georgia Institute of Technology, Atlanta, GA 30332-0150 USA (e-mail: wm.haddad@aerospace.gatech.edu; gtg891s@mail.gatech.edu).

J. M. Bailey is with the Department of Anesthesiology, Northeast Georgia Medical Center, Gainsville, GA 30503 USA (e-mail: james.bailey@nghs.com).

J. J. Im is with the Department of Mechanical Engineering, Virginia Institute of Technology, Blacksburg, VA 24061 USA (e-mail: jjim@vt.edu).

Digital Object Identifier 10.1109/TCST.2010.2042810

can be superimposed on the BIS score; and this undoubtedly contributes to the widespread use and value of the BIS device during surgery. However, to extend this technology outside of the operating room, or for that matter, to nonparalyzed patients in the operating room, further refinements are needed. In addition, if the BIS signal is to be used to quantify levels of consciousness for feedback control in general anesthesia, then the observation noise needs to be accounted for in the control system design process.

The challenge to the use of the BIS signal for closed-loop control of anesthesia is that the relationships between drug dose and tissue concentration (pharmacokinetics) and between tissue concentration and physiological effect (pharmacodynamics) is highly variable between individuals. In addition, observation noise in the BIS signal results in feedback measurement signals with high signal-to-noise ratios that need to be accounted for in the control algorithm. Adaptive feedback controllers seem particularly promising given this interpatient variability as well as BIS signal variation due to noise. In previous work, we have used nonnegative and compartmental dynamical systems theory to develop adaptive and neuroadaptive controllers for controlling the depth of anesthesia [11]–[13].

One of our initial efforts was the development of a direct adaptive control framework for uncertain nonlinear nonnegative and compartmental systems with nonnegative control inputs [11], [12]. This framework is Lyapunov-based and guarantees partial asymptotic set-point regulation, that is, asymptotic setpoint stability with respect to part of the closed-loop system states associated with the physiological state variables. In addition, the adaptive controllers, which are constructed without requiring knowledge of the pharmacokinetic and pharmacodynamic parameters, provide a nonnegative control input for stabilization with respect to a given setpoint in the nonnegative orthant. Subsequently, we also developed a neuroadaptive output feedback control framework for uncertain nonlinear nonnegative and compartmental systems with nonnegative control inputs [13], [14]. This framework is also Lyapunov-based and guarantees ultimate boundedness of the error signals corresponding to the physical system states in the face of interpatient pharmacokinetic and pharmacodynamic variability.

In a recent paper [15], we presented numerical and clinical results that compares and contrasts our adaptive control algorithm with our neural network adaptive control algorithm for controlling the depth of anesthesia in the operating theater during surgery. Specifically, 11 clinical trials were performed with our adaptive control algorithm [12] and seven clinical trials were performed with our neural network algorithm [13] at the Northeast Georgia Medical Center, Gainesville, GA. The proposed automated anesthesia controllers demonstrated excellent regulation of unconsciousness and allowed for a safe and effective administration of the anesthetic agent propofol. However, the adaptive and neuroadaptive controllers presented in [15] did not account for measurement noise in the EEG signal. Clinical testing has clearly demonstrated the need for developing adaptive and neuroadaptive controllers that can address system measurement noise [15].

In this paper, we extend the neuroadaptive controller framework developed in [13] and [14] to address measurement noise in the BIS signal. Specifically, we develop an output feedback neural network adaptive controller that operates over a tapped delay line (TDL) of available input and filtered output measurements. The neuroadaptive laws for the neural network weights are constructed using a linear observer for the nominal normal form error system dynamics. The proposed framework is Lyapunov-based and guarantees ultimate boundness of the error signals. In addition, the nonnegative neuroadaptive controller guarantees that the physiological system states remain in the nonnegative orthant of the state space. Finally, we present numerical and clinical results for controlling the depth of anesthesia in the operating theater during surgery. The proposed automated anesthesia neuroadaptive controller demonstrates excellent regulation of unconsciousness and allows for a safe and effective administration of the anesthetic agent propofol in the face of noisy EEG measurements.

II. Notation and Mathematical Preliminaries

In this section, we introduce notation, several definitions, and some key results concerning nonlinear nonnegative dynamical systems [16], [17] that are necessary for developing the main results of this paper. Specifically, for $x \in \mathbb{R}^n$ we write $x \geq\geq 0$ (respectively, $x \gg 0$) to indicate that every component of x is nonnegative (respectively, positive). In this case, we say that x is *nonnegative* or *positive*, respectively. Likewise, $A \in \mathbb{R}^{n\times m}$ is *nonnegative*[1] or *positive* if every entry of A is nonnegative or positive, respectively, which is written as $A \geq\geq 0$ or $A \gg 0$, respectively. Let $\overline{\mathbb{R}}_+^n$ and $\mathbb{R}_+^n$ denote the nonnegative and positive orthants of $\mathbb{R}^n$, that is, if $x \in \mathbb{R}^n$, then $x \in \overline{\mathbb{R}}_+^n$ and $x \in \mathbb{R}_+^n$ are equivalent, respectively, to $x \geq\geq 0$ and $x \gg 0$. Furthermore, we write $(\cdot)^{\mathrm{T}}$ to denote transpose, $\mathrm{tr}(\cdot)$ for the trace operator, $\lambda_{\min}(\cdot)$ to denote the minimum eigenvalue of a Hermitian matrix, $\|\cdot\|$ for a vector norm, $\|\cdot\|_{\mathrm{F}}$ for the Frobenius matrix norm, $\mathbf{e}$ to denote the ones vector of order n, that is, $\mathbf{e} \triangleq [1, \ldots, 1]^{\mathrm{T}}$, and $V'(x)$ for the Fréchet derivative of V at x. Finally, $M \otimes N$ denotes the Kronecker product of matrices M and N. The following definition introduces the notion of a nonnegative (respectively, positive) function.

Definition 2.1: Let $T > 0$. A real function $u : [0, T] \to \mathbb{R}^m$ is a *nonnegative* (respectively, *positive*) *function* if $u(t) \geq\geq 0$ (respectively, $u(t) \gg 0$) on the interval $[0, T]$.

The following definition introduces the notion of essentially nonnegative and compartmental vector fields [17].

Definition 2.2: Let $f = [f_1, \ldots, f_n]^{\mathrm{T}} : \mathcal{D} \subseteq \overline{\mathbb{R}}_+^n \to \mathbb{R}^n$. Then f is *essentially nonnegative* if $f_i(x) \geq 0$, for all $i = 1, \ldots, n$, and $x \in \overline{\mathbb{R}}_+^n$ such that $x_i = 0$, where x_i denotes the ith component of x. f is *compartmental* if f is essentially nonnegative and $\mathbf{e}^{\mathrm{T}} f(x) \leq 0$, $x \in \overline{\mathbb{R}}_+^n$.

Note that if $f(x) = Ax$, where $A \in \mathbb{R}^{n\times n}$, then f is essentially nonnegative if and only if A is essentially nonnegative, that is, $A_{(i,j)} \geq 0$, $i, j = 1, \ldots, n$, $i \neq j$, where $A_{(i,j)}$ denotes the (i, j)th entry of A.

[1]In this paper it is important to distinguish between a square nonnegative (respectively, positive) matrix and a nonnegative-definite (respectively, positive-definite) matrix.

In this paper, we consider controlled nonlinear dynamical systems of the form

$$\dot{x}(t) = f(x(t)) + G(x(t))u(t), \quad x(0) = x_0, \quad t \geq 0 \tag{1}$$

where $x(t) \in \mathbb{R}^n$, $t \geq 0$, $u(t) \in \mathbb{R}^m$, $t \geq 0$, $f : \mathbb{R}^n \to \mathbb{R}^n$ is locally Lipschitz continuous and satisfies $f(0) = 0$, $G : \mathbb{R}^n \to \mathbb{R}^{n\times m}$ is continuous, and $u : [0, \infty) \to \mathbb{R}^m$ is piecewise continuous.

The following definition and proposition are needed for the main results of this paper.

Definition 2.3: The nonlinear dynamical system given by (1) is *nonnegative* if for every $x(0) \in \overline{\mathbb{R}}^n_+$ and $u(t) \geq\geq 0$, $t \geq 0$, the solution $x(t)$, $t \geq 0$, to (1) is nonnegative.

Proposition 2.1 [17]: The nonlinear dynamical system given by (1) is nonnegative if $f : \mathbb{R}^n \to \mathbb{R}^n$ is essentially nonnegative and $G(x) \geq\geq 0$, $x \in \overline{\mathbb{R}}^n_+$.

It follows from Proposition 2.1 that if $f(\cdot)$ is essentially nonnegative, then a nonnegative input signal $G(x(t))u(t)$, $t \geq 0$, is sufficient to guarantee the nonnegativity of the state of (1).

III. Neuroadaptive Output Feedback Control for Nonlinear Nonnegative Uncertain Systems

In this section, we consider the problem of characterizing neuroadaptive dynamic output feedback control laws for nonlinear nonnegative and compartmental uncertain dynamical systems to achieve *set-point* regulation in the nonnegative orthant. Specifically, consider the controlled square (i.e., the number of inputs is equal to the number of outputs) nonlinear uncertain dynamical system $\mathcal{G}$ given by

$$\dot{x}(t) = f(x(t)) + G(x(t))u(t), \; x(0) = x_0, \; t \geq 0 \tag{2}$$
$$y(t) = h(x(t)) \tag{3}$$
$$y_n(t) = y(t) + n(t) \tag{4}$$

where $x(t) \in \mathbb{R}^n$, $t \geq 0$, is the state vector, $u(t) \in \mathbb{R}^m$, $t \geq 0$, is the control input, $y(t) \in \mathbb{R}^m$, $t \geq 0$, is the system output, $y_n(t) \in \mathbb{R}^m$, $t \geq 0$, is the noisy system output, $n(t) \in \mathbb{R}^m$, $t \geq 0$, is a noise signal such that $\|n(t)\| \leq n^* < \infty$, for all $t \geq 0$, $f : \mathbb{R}^n \to \mathbb{R}^n$ is essentially nonnegative but otherwise unknown, $G : \mathbb{R}^n \to \mathbb{R}^{n\times m}$ is an unknown nonnegative input matrix function, and $h : \mathbb{R}^n \to \mathbb{R}^m$ is a nonnegative output function. We assume that $f(\cdot)$, $G(\cdot)$, and $h(\cdot)$ are smooth (at least C^n mappings) and the control input $u(\cdot)$ in (2) is restricted to the class of *admissible controls* consisting of measurable functions such that $u(t) \in \mathbb{R}^m$, $t \geq 0$. Furthermore, we assume that the distribution spanned by the vector fields composed by the column vectors of $G(x)$, $x \in \mathbb{R}^n$, has a constant dimension and is involutive in a neighborhood of the equilibrium point of (2).

As discussed in the Introduction, control (source) inputs of drug delivery systems for physiological and pharmacological processes are usually constrained to be nonnegative as are the system states. Hence, in this paper we develop neuroadaptive dynamic output feedback control laws for nonnegative systems with nonnegative control inputs. Specifically, for a given desired set point $y_d \in \overline{\mathbb{R}}^m_+$ and for a given $\varepsilon > 0$, our aim is to design a nonnegative control input $u(t)$, $t \geq 0$, predicated on the system measurement $y_n(t)$, $t \geq 0$, such that $\|y(t) - y_d\| < \varepsilon$, for all $t \geq T$, where $T \in [0, \infty)$, and $x(t) \geq\geq 0$, $t \geq 0$, for all $x_0 \in \overline{\mathbb{R}}^n_+$.

In this paper, we assume that for the nonlinear dynamical system (2) and (3), the conditions for the existence of a globally defined diffeomorphism transforming (2) and (3) into a normal form [18], [19] are satisfied. Specifically, we assume that there exist a global diffeomorphism $\mathcal{T} : \mathbb{R}^n \to \mathbb{R}^n$ and C^n functions $f_\xi : \mathbb{R}^r \times \mathbb{R}^{n-r} \to \mathbb{R}^r$ and $f_z : \mathbb{R}^r \times \mathbb{R}^{n-r} \to \mathbb{R}^{n-r}$ such that, in the coordinates $\left[\xi^{\mathrm{T}},\ z^{\mathrm{T}}\right]^{\mathrm{T}} \triangleq \mathcal{T}(x)$, where

$$\xi \triangleq [y_1, \dot{y}_1, \ldots, y_1^{(r_1-2)}, \ldots, y_m, \dot{y}_m, \ldots, y_m^{(r_m-2)};\ y_1^{(r_1-1)}, \ldots, y_m^{(r_m-1)}] \in \mathbb{R}^r$$

$y_i^{(r_i)}$ denotes the r_ith derivative of y_i, r_i denotes the relative degree of $\mathcal{G}$ with respect to the output y_i, $z \in \mathbb{R}^{n-r}$, and $r \triangleq r_1 + \cdots + r_m$ is the (vector) relative degree of $\mathcal{G}$, the nonlinear dynamical system $\mathcal{G}$ given by (2)–(4) is equivalent to

$$\dot{\xi}(t) = f_\xi(\xi(t), z(t)) + G_\xi(\xi(t), z(t))u(t), \; \xi(0) = \xi_0, \; t \geq 0 \tag{5}$$
$$\dot{z}(t) = f_z(\xi(t), z(t)), \quad z(0) = z_0 \tag{6}$$
$$y(t) = C\xi(t) \tag{7}$$
$$y_n(t) = C\xi(t) + n(t) \tag{8}$$

where $\xi(t) \in \mathbb{R}^r$, $t \geq 0$, $z(t) \in \mathbb{R}^{n-r}$, $t \geq 0$

$$f_\xi(\xi, z) = A\xi + \tilde{f}_{\mathrm{u}}(\xi, z), \; G_\xi(\xi, z) = \begin{bmatrix} 0_{(\mathrm{r}-m)\times m} \\ \hat{G}(\tilde{x}) \end{bmatrix} \tag{9}$$

$$A = \begin{bmatrix} A_0 \\ \hat{A} \end{bmatrix}, \quad \tilde{f}_{\mathrm{u}}(\xi, z) = \begin{bmatrix} 0_{(\mathrm{r}-m)\times 1} \\ f_{\mathrm{u}}(\tilde{x}) \end{bmatrix} \tag{10}$$

$\tilde{x} \triangleq [\xi^{\mathrm{T}}, z^{\mathrm{T}}]^{\mathrm{T}}$, $A_0 \in \mathbb{R}^{(r-m)\times r}$ is a known matrix of zeros and ones capturing the multivariable observable canonical form representation [20], $\hat{A} \in \mathbb{R}^{m\times r}$ is such that A is asymptotically stable, $f_{\mathrm{u}} : \mathbb{R}^n \to \mathbb{R}^m$ is an unknown function, $C \in \mathbb{R}^{m\times r}$ is a known matrix of zeros and ones capturing the system output, and $\hat{G} : \mathbb{R}^n \to \mathbb{R}^{m\times m}$ is an unknown matrix function such that $\det \hat{G}(\tilde{x}) \neq 0$, $\tilde{x} \in \mathbb{R}^n$. Furthermore, we assume that for a given $y_{\mathrm{d}} \in \overline{\mathbb{R}}^m_+$ there exist $z_e \in \mathbb{R}^{n-r}$ and $u_e \in \overline{\mathbb{R}}^m_+$ such that $x_e \triangleq \mathcal{T}^{-1}(\tilde{x}_e) \geq\geq 0$ and

$$0 = f_\xi(\xi_e, z_e) + G_\xi(\xi_e, z_e)u_e \tag{11}$$
$$0 = f_z(\xi_e, z_e) \tag{12}$$

where $\tilde{x}_e \triangleq [\xi_e^{\mathrm{T}}, z_e^{\mathrm{T}}]^{\mathrm{T}}$ and ξ_e is given with $y_i = y_{\mathrm{d}i}$, $i = 1, \ldots, m$, and $\dot{y}_i = \cdots = y_i^{(r_i-1)} = 0$, $i = 1, \ldots, m$. As we see in Section IV, the aforementioned assumptions are automatically satisfied for our clinical compartmental model.

To ensure that for a bounded state $\xi(t)$, $t \geq 0$, the dynamics given by (6) are bounded, we assume that (6) is input-to-state stable at $z(t) \equiv z_e$ with $\xi(t) - \xi_e$ viewed as the input; that is, there exist a class $\mathcal{KL}$ function $\eta(\cdot, \cdot)$ and a class $\mathcal{K}$ function $\gamma(\cdot)$ such that

$$\|z(t) - z_e\| \leq \eta(\|z_0 - z_e\|, t) + \gamma\left(\sup_{0\leq\tau\leq t} \|\xi(\tau) - \xi_e\|\right) \tag{13}$$

where $\|\cdot\|$ denotes the Euclidean vector norm. Unless otherwise stated, henceforth we use $\|\cdot\|$ to denote the Euclidean vector norm. Note that $(\xi_e, z_e) \in \mathbb{R}^r \times \mathbb{R}^{n-r}$ is an equilibrium point

of (5) and (6) if and only if there exists $u_e \in \overline{\mathbb{R}}_+^m$ such that (11) and (12) hold.

Finally, we assume that the functions $f_{\rm u}(\mathcal{T}(x)) - f_{\rm u}(\mathcal{T}(x_e)) - \hat{G}(\mathcal{T}(x_e))u_e$ and $\hat{G}(\mathcal{T}(x)) - \hat{B}$, where $\hat{B} \in \mathbb{R}^{m\times m}$, can be approximated over a compact set $\mathcal{D}_{\rm c} \subset \overline{\mathbb{R}}_+^n$ by a linear in the parameters neural network up to a desired accuracy. In this case, there exist $\varepsilon_1 : \mathbb{R}^n \to \mathbb{R}^m$ and $\varepsilon_2 : \mathbb{R}^n \to \mathbb{R}^{m\times m}$ such that $\|\varepsilon_1(x)\| < \varepsilon_1^*$ and $\|\varepsilon_2(x)\|_{\rm F} < \varepsilon_2^*$, $x \in \mathcal{D}_{\rm c}$, where $\varepsilon_1^* > 0$ and $\varepsilon_2^* > 0$, and

$$f_{\rm u}(\mathcal{T}(x)) - f_{\rm u}(\mathcal{T}(x_e)) - \hat{G}(\mathcal{T}(x_e))u_e = W_1^{\rm T}\hat{\sigma}_1(x) + \varepsilon_1(x) \quad (14)$$

$$\hat{G}(\mathcal{T}(x)) - \hat{B} = W_2^{\rm T}[I_m \otimes \hat{\sigma}_2(x)] + \varepsilon_2(x) \quad (15)$$

where $x \in \mathcal{D}_{\rm c}$, $W_1 \in \mathbb{R}^{s_1\times m}$ and $W_2 \in \mathbb{R}^{ms_2\times m}$ are optimal *unknown* (constant) weights that minimize the approximation errors over $\mathcal{D}_{\rm c}$, $\hat{\sigma}_1 : \mathbb{R}^n \to \mathbb{R}^{s_1}$ and $\hat{\sigma}_2 : \mathbb{R}^n \to \mathbb{R}^{s_2}$ are basis functions such that each component of $\hat{\sigma}_1(\cdot)$ and $\hat{\sigma}_2(\cdot)$ takes values between 0 and 1, and $\varepsilon_1(\cdot)$ and $\varepsilon_2(\cdot)$ are the modeling errors. Note that $s_1 + s_2$ denotes the total number of basis functions or, equivalently, the number of nodes of the neural network.

Since $f_{\rm u}(\cdot)$ and $\hat{G}(\cdot)$ are continuous, we can choose $\hat{\sigma}_1(\cdot)$ and $\hat{\sigma}_2(\cdot)$ from a linear space $\mathcal{X}$ of continuous functions that forms an algebra and separates points in $\mathcal{D}_{\rm c}$. In this case, it follows from the Stone–Weierstrass theorem [21, p. 212] that $\mathcal{X}$ is a dense subset of the set of continuous functions on $\mathcal{D}_{\rm c}$. Now, as is the case in the standard neuroadaptive control literature [22], we can construct the signal $u_{\rm ad} = F(\hat{W}_1, \hat{W}_2, \hat{\sigma}_1(x), \hat{\sigma}_2(x))$, where $F : \mathbb{R}^{s_1\times m} \times \mathbb{R}^{ms_2\times m} \times \mathbb{R}^{s_1} \times \mathbb{R}^{s_2} \to \mathbb{R}^m$, involving the estimates of the optimal weights and basis functions as our adaptive control signal. It is important to note here that we assume that we know both the structure and the size of the approximator. This is a standard assumption in the neural network adaptive control literature. In online neural network training, the size and the structure of the optimal approximator are not known and are often chosen by the rule that the larger the size of the neural network and the richer the distribution class of the basis functions over a compact domain, the tighter the resulting approximation error bounds ε_1^* and ε_2^*. This goes back to the Stone–Weierstrass theorem which only provides an existence result without any constructive guidelines.

Since the actual measurement $y_n(t)$, $t \geq 0$, is noisy with $n(t)$, $t \geq 0$, representing a high-frequency noise signal, we use a filtered version of $y_n(t)$, $t \geq 0$, in the control input $u(t)$, $t \geq 0$. Specifically, we design an asymptotically stable low-pass filter of the form

$$\dot{x}_{\rm f}(t) = A_{\rm f}x_{\rm f}(t) + B_{\rm f}y_n(t), \quad x_{\rm f}(0) = x_{\rm f_0}, \quad t \geq 0 \quad (16)$$

$$y_{\rm f}(t) = C_{\rm f}x_{\rm f}(t) \quad (17)$$

where $A_{\rm f} \in \mathbb{R}^{n_{\rm f}\times n_{\rm f}}$ is Hurwitz and $B_{\rm f} \in \mathbb{R}^{n_{\rm f}\times m}$ and $C_{\rm f} \in \mathbb{R}^{m\times n_{\rm f}}$ are such that $\lim_{\omega\to\infty}|G_{(i,j)}(\jmath\omega)| = 0$, $i, j = 1, \ldots, m$, where $G_{(i,j)}(s)$ denotes the (i,j)th entry of the transfer function $G(s) \triangleq C_{\rm f}(sI_{n_{\rm f}} - A_{\rm f})^{-1}B_{\rm f}$. Here, we choose the matrices $A_{\rm f}$, $B_{\rm f}$, and $C_{\rm f}$ such that $C_{\rm f}A_{\rm f}^{-1}B_{\rm f} = -I_m$. In this case, for every $y_{\rm d} \in \overline{\mathbb{R}}_+^m$, there exists $x_{\rm f_e} \in \mathbb{R}^{n_{\rm f}}$ such that

$$0 = A_{\rm f}x_{\rm f_e} + B_{\rm f}y_{\rm d} \quad (18)$$

$$y_{\rm d} = C_{\rm f}x_{\rm f_e}. \quad (19)$$

Note that since $A_{\rm f}$ is Hurwitz there exist positive-definite matrices $\hat{P} \in \mathbb{R}^{n_{\rm f}\times n_{\rm f}}$ and $\hat{R} \in \mathbb{R}^{n_{\rm f}\times n_{\rm f}}$ such that

$$0 = A_{\rm f}^{\rm T}\hat{P} + \hat{P}A_{\rm f} + \hat{R}. \quad (20)$$

In order to develop an *output* feedback neural network, we use the recent approach developed in [23] for reconstructing the system states via the system delayed inputs and filtered outputs. Specifically, we use a *memory unit* as a particular form of a tapped delay line that takes a scalar time series input and provides an $(2mn-r)$-dimensional vector output consisting of the present values of the system filtered outputs and system inputs, and their $2(n-1)m - r$ delayed values given by

$$\begin{aligned}\zeta(t) \triangleq [&y_{{\rm f}_1}(t), y_{{\rm f}_1}(t-d), \ldots, y_{{\rm f}_1}(t-(n-1)d),\\ &\ldots, y_{{\rm f}_m}(t), y_{{\rm f}_m}(t-d), \ldots, y_{{\rm f}_m}(t-(n-1)d);\\ &u_1(t), u_1(t-d), \ldots, u_1(t-(n-r_1-1)d),\\ &\ldots, u_m(t), u_m(t-d), \ldots, u_m(t-(n-r_m-1)d)]^{\rm T},\\ &t \geq 0\end{aligned} \quad (21)$$

where $d > 0$.

For the statement of our main result, define the projection operator $\mathrm{Proj}(\tilde{W}, Y)$ given by the equation shown at the bottom of the page, where $\tilde{W} \in \mathbb{R}^{s\times m}$, $Y \in \mathbb{R}^{n\times m}$, $\mu(\tilde{W}) \triangleq (\mathrm{tr}\,\tilde{W}^{\rm T}\tilde{W} - \tilde{w}_{\max}^2)/\varepsilon_{\tilde{W}}$, $\tilde{w}_{\max} \in \mathbb{R}$ is the norm bound imposed on $\tilde{W}$, and $\varepsilon_{\tilde{W}} > 0$. Note that for a given matrix $\tilde{W} \in \mathbb{R}^{s\times m}$ and $Y \in \mathbb{R}^{n\times m}$, it follows that

$$\begin{aligned}&\mathrm{tr}[(\tilde{W} - W)^{\rm T}(\mathrm{Proj}(\tilde{W}, Y) - Y)]\\ &= \sum_{i=1}^{n}[\mathrm{col}_i(\tilde{W} - W)]^{\rm T}[\mathrm{Proj}(\mathrm{col}_i(\tilde{W}), \mathrm{col}_i(Y)) - \mathrm{col}_i(Y)]\\ &\leq 0\end{aligned} \quad (22)$$

where $\mathrm{col}_i(X)$ denotes the ith column of the matrix X.

Assumption 3.1: For a given $y_{\rm d} \in \overline{\mathbb{R}}_+^m$ assume there exist nonnegative vectors $x_e \in \overline{\mathbb{R}}_+^n$ and $u_e \in \overline{\mathbb{R}}_+^m$ such that

$$0 = f(x_e) + G(x_e)u_e \quad (23)$$

$$y_{\rm d} = h(x_e). \quad (24)$$

$$\mathrm{Proj}(\tilde{W}, Y) \triangleq \begin{cases} Y, & \text{if } \mu(\tilde{W}) < 0,\\ Y, & \text{if } \mu(\tilde{W}) \geq 0 \text{ and } \mu'(\tilde{W})Y \leq 0,\\ Y - \frac{\mu'^{\rm T}(\tilde{W})\mu'(\tilde{W})Y}{\mu'(\tilde{W})\mu'^{\rm T}(\tilde{W})}\mu(\tilde{W}), & \text{otherwise}\end{cases}$$

Furthermore, assume that the equilibrium point x_e of (2) is globally asymptotically stable and nonnegative with $u(t) \equiv u_e$. Finally, assume that there exists a global diffeomorphism $\mathcal{T} : \mathbb{R}^n \to \mathbb{R}^n$ such that $\mathcal{G}$ can be transformed into the normal form given by (5) and (6), and (6) is input-to-state stable at z_e with $\xi(t) - \xi_e$ viewed as the input.

Consider the neuroadaptive output feedback control law given by

$$u(t) = \begin{cases} \hat{u}(t), & \text{if } \hat{u}(t) \geq\geq 0 \\ 0, & \text{otherwise} \end{cases} \tag{25}$$

where

$$\hat{u}(t) = -\left(\hat{B} + \hat{W}_2^{\mathrm{T}}(t)[I_m \otimes \sigma_2(\zeta(t))]\right)^{-1} \hat{W}_1^{\mathrm{T}}(t)\sigma_1(\zeta(t)) \tag{26}$$

$\hat{B} \in \mathbb{R}^{m\times m}$ is nonsingular, $\zeta(t)$, $t \geq 0$, is given by (21), $\sigma_1 : \mathbb{R}^n \to \mathbb{R}^{s_1}$ and $\sigma_2 : \mathbb{R}^n \to \mathbb{R}^{s_2}$ are basis functions such that each component of $\sigma_1(\cdot)$ and $\sigma_2(\cdot)$ takes values between 0 and 1, $\hat{W}_1(t) \in \mathbb{R}^{s_1\times m}$, $t \geq 0$, and $\hat{W}_2(t) \in \mathbb{R}^{ms_2\times m}$, $t \geq 0$. Here, the update laws satisfy

$$\dot{\hat{W}}_1(t) = Q_1 \mathrm{Proj}[\hat{W}_1(t), -\sigma_1(\zeta(t))\xi_{\mathrm{c}}^{\mathrm{T}}(t)\tilde{P}B_0] \qquad \hat{W}_1(0) = \hat{W}_{10}, \quad t \geq 0 \tag{27}$$

$$\dot{\hat{W}}_2(t) = Q_2 \mathrm{Proj}[\hat{W}_2(t), -[I_m \otimes \sigma_2(\zeta(t))]u(t)\xi_{\mathrm{c}}^{\mathrm{T}}(t)\tilde{P}B_0] \qquad \hat{W}_2(0) = \hat{W}_{20}, \quad t \geq 0 \tag{28}$$

where $Q_1 \in \mathbb{R}^{s_1\times s_1}$ and $Q_2 \in \mathbb{R}^{ms_2\times ms_2}$ are positive definite matrices, $\tilde{P} \in \mathbb{R}^{r\times r}$ is a positive-definite solution of the Lyapunov equation

$$0 = (A - LC)^{\mathrm{T}}\tilde{P} + \tilde{P}(A - LC) + \tilde{R} \tag{29}$$

where $\tilde{R} > 0$, and $\xi_{\mathrm{c}}(t)$, $t \geq 0$, is the solution to the estimator dynamics

$$\dot{\xi}_{\mathrm{c}}(t) = A\xi_{\mathrm{c}}(t) + L(y_{\mathrm{f}}(t) - y_{\mathrm{c}}(t) - y_{\mathrm{d}}), \quad \xi_{\mathrm{c}}(0) = \xi_{\mathrm{c}0}, \quad t \geq 0 \tag{30}$$

$$y_{\mathrm{c}}(t) = C\xi_{\mathrm{c}}(t) \tag{31}$$

where $\xi_{\mathrm{c}}(t) \in \mathbb{R}^r$, $t \geq 0$, $A \in \mathbb{R}^{r\times r}$ is given by (10), $L \in \mathbb{R}^{r\times m}$ is such that $A - LC$ is Hurwitz, $y_{\mathrm{f}}(t)$, $t \geq 0$, is the output of the filter (16) and (17), and $B_0 \triangleq [0_{m\times(\mathrm{r}-m)}, I_m]^{\mathrm{T}}$. For the statement of the next result recall the definition of ultimate boundedness given in [24, p. 241].

Theorem 3.1: Consider the nonlinear uncertain dynamical system $\mathcal{G}$ given by (2) and (3) with $u(t)$, $t \geq 0$, given by (25). Assume Assumption 3.1 holds, $\lambda_{\min}(RP^{-1}) > 1$, $\lambda_{\min}(\tilde{R}\tilde{P}^{-1}) > 1$, and $\lambda_{\min}(\hat{R}) > \|\hat{P}B_{\mathrm{f}}CP^{-1/2}\|$, where $\hat{P} \in \mathbb{R}^{n_{\mathrm{f}}\times n_{\mathrm{f}}}$, $\tilde{P} \in \mathbb{R}^{r\times r}$, and $P \in \mathbb{R}^{r\times r}$ are the positive-definite solutions of the Lyapunov (20), (29), and

$$0 = A^{\mathrm{T}}P + PA + R \tag{32}$$

where $R > 0$. Then there exists a compact positively invariant set $\mathcal{D}_\alpha \subset \mathbb{R}^n \times \mathbb{R}^r \times \mathbb{R}^{s_1\times m} \times \mathbb{R}^{ms_2\times m} \times \mathbb{R}^{n_{\mathrm{f}}}$ such that $(x_e, 0, W_1, W_2, x_{\mathrm{f}_e}) \in \mathcal{D}_\alpha$, where $W_1 \in \mathbb{R}^{s_1\times m}$ and $W_2 \in \mathbb{R}^{ms_2\times m}$, and the solution $(x(t), \xi_{\mathrm{c}}(t), \hat{W}_1(t), \hat{W}_2(t), x_{\mathrm{f}}(t))$, $t \geq 0$, of the closed-loop system given by (2), (16), (17), (25), (27), (28), (30), and (31) is ultimately bounded for all $(x(0), \xi_{\mathrm{c}}(0), \hat{W}_1(0), \hat{W}_2(0), x_{\mathrm{f}}(0)) \in \mathcal{D}_\alpha$ with ultimate bound $\|y(t) - y_{\mathrm{d}}\|^2 < \varepsilon$, $t \geq T$, where

$$\begin{aligned} \varepsilon > \Big[&(\nu^{1/2}(\lambda_{\min}(RP^{-1}) - 1)^{-1/2} + \alpha_1)^2 \\ &+ (\nu^{1/2}\lambda_{\min}^{-1/2}(\tilde{R}\tilde{P}^{-1}) + \alpha_2)^2 \\ &+ (\nu^{1/2}(\lambda_{\min}(\hat{R}) - \|\hat{P}B_{\mathrm{f}}CP^{-1/2}\|)^{-1/2} + \alpha_3)^2 \\ &+ \lambda_{\max}(Q_1^{-1})\hat{w}_{1\max}^2 + \lambda_{\max}(Q_2^{-1})\hat{w}_{2\max}^2\Big]^{1/2} \end{aligned} \tag{33}$$

$$\begin{aligned} \nu \triangleq\ &(\lambda_{\min}(RP^{-1}) - 1)\alpha_1^2 + \lambda_{\min}(\tilde{R}\tilde{P}^{-1})\alpha_2^2 \\ &+ \left(\lambda_{\min}(\hat{R}) - \|\hat{P}B_{\mathrm{f}}CP^{-1/2}\|\right)\alpha_3^2 \end{aligned} \tag{34}$$

$$\begin{aligned} \alpha_1 \triangleq\ &\Big(\|P^{-1/2}(P + \tilde{P})B_0\|[\sqrt{s_1}\hat{w}_{1\max} + \sqrt{ms_2}\hat{w}_{2\max}u^*] \\ &+ (2\sqrt{s_1}\hat{w}_{1\max} + \sqrt{ms_2}\hat{w}_{2\max}u^* \\ &+ \varepsilon_1^* + \varepsilon_2^*u^*)\|P^{1/2}B_0\|\Big)(\lambda_{\min}(RP^{-1}) - 1)^{-1} \end{aligned} \tag{35}$$

$$\begin{aligned} \alpha_2 \triangleq\ &\lambda_{\min}^{-1}(\tilde{R}\tilde{P}^{-1})\Big[2\sqrt{s_1}\hat{w}_{1\max} + \sqrt{ms_2}\hat{w}_{2\max}u^* \\ &+ (\varepsilon_1^* + \varepsilon_2^*u^*)\Big]\|\tilde{P}^{1/2}B_0\| \end{aligned} \tag{36}$$

$$\alpha_3 \triangleq n^*\|\hat{P}B_{\mathrm{f}}\|\left(\lambda_{\min}(\hat{R}) - \|\hat{P}B_{\mathrm{f}}CP^{-1/2}\|\right)^{-1} \tag{37}$$

$u^* \triangleq \sup_{t\geq 0}\|u(t)\|$, $\hat{w}_{i\max}$, $i = 1, 2$, are norm bounds imposed on $\hat{W}_i$, and $\tilde{P} \in \mathbb{R}^{r\times r}$ is the positive-definite solution of the Lyapunov (29). Furthermore, $u(t) \geq\geq 0$, $t \geq 0$, and $x(t) \geq\geq 0$, $t \geq 0$, for all $x_0 \in \overline{\mathbb{R}}_+^n$.

Proof: The proof is given in the Appendix . □

Remark 3.1: If in Theorem 3.1 $\lambda_{\min}(RP^{-1}) > 1$ is not satisfied for a given A, we can modify (9) as $f_\xi(\xi, z) = \bar{A}\xi + \bar{f}_{\mathrm{u}}(\xi, z)$, where $\bar{f}_{\mathrm{u}}(\xi, z) = \tilde{f}_{\mathrm{u}}(\xi, z) + (A - \bar{A})\xi$ and $\bar{A}$ is such that $\lambda_{\min}(\bar{R}\bar{P}^{-1}) > 1$, where

$$0 = \bar{A}^{\mathrm{T}}\bar{P} + \bar{P}\bar{A} + \bar{R}.$$

For example, with $\bar{A} = -\alpha I_n$, where $\alpha > 1/2$, $\lambda_{\min}(\bar{R}\bar{P}^{-1}) > 1$ is guaranteed. In this case, Theorem 3.1 holds with A replaced by $\bar{A}$. In addition, by properly choosing L we can ensure that $\lambda_{\min}(\tilde{R}\tilde{P}^{-1}) > 1$. Finally, choosing B_{f} small enough and independent of $\hat{R}$, $\hat{P}$, C, and P, $\lambda_{\min}(\hat{R}) > \|\hat{P}B_{\mathrm{f}}CP^{-1/2}\|$ can also be guaranteed.

Remark 3.2: The domain of attraction $\mathcal{D}_\alpha$ in Theorem 3.1 is given by (67) and is characterized by the Lyapunov-like function (52) that guarantees ultimate boundedness for the closed-loop system. For details see the Appendix.

A block diagram showing the neuroadaptive control architecture given in Theorem 3.1 is shown in Fig. 1. It is important to note that the existence of a global neural network approximator for an uncertain nonlinear map using the system filtered outputs and inputs, and its delayed values cannot in general be established. In the proof of Theorem 3.1 (see the Appendix), as is common in the neural network literature, we assume that for a given arbitrarily large compact set $\mathcal{D}_{\mathrm{c}} \subset \mathbb{R}^n$, there exists an approximator for the unknown nonlinear map up to a desired accuracy. This assumption ensures that in the error space $\tilde{\mathcal{D}}_e$ defined in the Appendix, there exists at least one Lyapunov level set such that

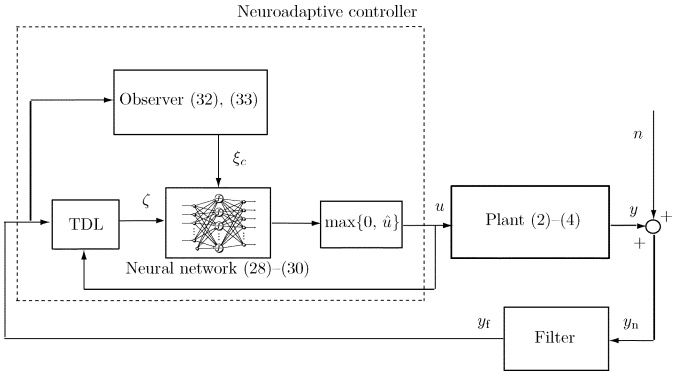

Fig. 1. Block diagram of the closed-loop system.

the set inclusions invoked in the proof of Theorem 3.1 are satisfied. In the case where $f_{\rm u}(\cdot)$ and $\hat{G}(\cdot)$ are continuous on $\mathbb{R}^n$, it follows from the Stone–Weierstrass theorem that $f_{\rm u}(\cdot)$ and $\hat{G}(\cdot)$ can be approximated over an arbitrarily large compact set $\mathcal{D}_{\rm c}$ in the sense of (14) and (15). Finally, we note that since the norm of $\hat{W}_2(t)$ is bounded it is always possible to choose $\hat{B}$ so that $(\hat{B} + \hat{W}_2^{\rm T}(t)[I_m \otimes \sigma_2(\zeta(t))])^{-1}$ exists and is bounded for all $t \geq 0$ so that there exists $u^* > 0$ such that $u^* \geq \|u(t)\|, t \geq 0$. This follows from the fact that for any two square matrices A and B, $\det(A + B) \neq 0$ if and only if there exists $\alpha > 0$ such that $\sigma_{\min}(A) > \alpha$ and $\sigma_{\max}(B) \leq \alpha$, where $\sigma_{\min}(\cdot)$ and $\sigma_{\max}(\cdot)$ denote the minimum and maximum singular value, respectively.

Implementing the neuroadaptive controller (26) requires a fixed-point iteration at each integration step, that is, the controller contains an algebraic constraint on u. For each choice of $\sigma_1(\cdot)$ and $\sigma_2(\cdot)$ this equation must be examined for solvability in terms of u. It is more practical to avoid this iteration by using one-step delayed values of u in calculating $\hat{u}$. Implementations using both approaches result in imperceptible differences in our numerical studies.

In Theorem 3.1 we assumed that the equilibrium point x_e of (2) is globally asymptotically stable with $u(t) \equiv u_e$. In general, however, unlike linear nonnegative systems with asymptotically stable plant dynamics, a given set point $x_e \in \mathbb{R}_+^n$ for the nonlinear nonnegative dynamical system (2) may not be asymptotically stablizable with a constant control $u(t) \equiv u_e \in \overline{\mathbb{R}}_+^m$. However, if $f(x)$ is homogeneous, cooperative, that is, the Jacobian matrix $\partial f(x)/\partial x$ is essentially nonnegative for all $x \in \overline{\mathbb{R}}_+^n$, the Jacobian matrix $\partial f(x)/\partial x$ is irreducible for all $x \in \overline{\mathbb{R}}_+^n$ [16], and the zero solution $x(t) \equiv 0$ of the undisturbed ($u(t) \equiv 0$) system (2) is globally asymptotically stable, then the set point $x_e \in \mathbb{R}_+^n$ satisfying (11) and (12) is a unique equilibrium point with $u(t) \equiv u_e$ and is also asymptotically stable for all $x_0 \in \overline{\mathbb{R}}_+^n$ [25], [26]. This implies that the solution $x(t) \equiv x_e$ to (2) with $u(t) \equiv u_e$ is asymptotically stable for all $x_0 \in \overline{\mathbb{R}}_+^n$.

IV. Neuroadaptive Output Feedback Control for General Anesthesia

Almost all anesthetics are *myocardial* depressants, that is, they decrease the contractility of the heart and lower *cardiac output* (i.e., the volume of blood pumped by the heart per unit time). As a consequence, decreased cardiac output slows down redistribution kinetics, that is, the transfer of blood from the central compartment (heart, brain, kidney, and liver) to the peripheral compartments (muscle and fat). In addition, decreased

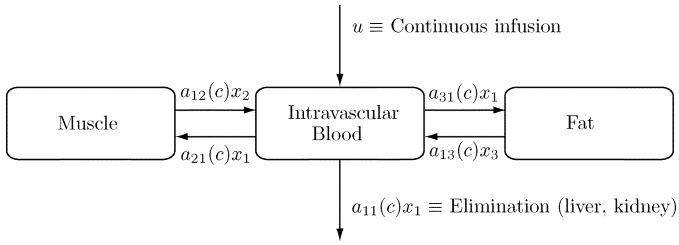

Fig. 2. Pharmacokinetic model for drug distribution during anesthesia.

cardiac output could increase drug concentrations in the central compartment, causing even more myocardial depression and further decrease in cardiac output. This instability can lead to overdosing that, at the very least, can delay recovery from anesthesia and, in the worst case, can result in respiratory and cardiovascular collapse. Alternatively, underdosing can result in patients psychologically traumatized by pain and awareness during surgery. Thus, control of drug effect is clinically important since overdosing or underdosing incur risk for the patient.

To illustrate the application of the neuroadaptive control framework presented in Section III for general anesthesia we develop a model for the intravenous anesthetic propofol. The pharmacokinetics of propofol are described by the three compartment model [12], [27] shown in Fig. 2, where x_1 denotes the mass of drug in the central compartment, which is the site for drug administration and is generally thought to be comprised of the *intravascular blood* volume (blood within arteries and veins) as well as *highly perfused* organs (organs with high ratios of blood flow to weight) such as the heart, brain, kidney, and liver. These organs receive a large fraction of the cardiac output. The remainder of the drug in the body is assumed to reside in two peripheral compartments, one identified with muscle and one with fat; the masses in these compartments are denoted by x_2 and x_3, respectively. These compartments receive less than 20% of the cardiac output.

A mass balance of the three-state compartmental model yields

$$\begin{aligned}\dot{x}_1(t) = &-[a_{11}(c(t)) + a_{21}(c(t)) + a_{31}(c(t))]x_1(t)\\ &+ a_{12}(c(t))x_2(t) + a_{13}(c(t))x_3(t) + u(t)\\ &x_1(0) = x_{10}, \quad t \geq 0 \qquad (38)\\ \dot{x}_2(t) = &\, a_{21}(c(t))x_1(t) - a_{12}(c(t))x_2(t)\\ &x_2(0) = x_{20}, \quad t \geq 0 \qquad (39)\\ \dot{x}_3(t) = &\, a_{31}(c(t))x_1(t) - a_{13}(c(t))x_3(t)\\ &x_3(0) = x_{30}, \quad t \geq 0 \qquad (40)\end{aligned}$$

where $c(t) = x_1(t)/V_{\rm c}$, $V_{\rm c}$ is the volume of the central compartment (about 15 l for a 70 kg patient), $a_{ij}(c)$, $i \neq j$, is the rate of transfer of drug from the jth compartment to the ith compartment, $a_{11}(c)$ is the rate of drug metabolism and elimination (metabolism typically occurs in the liver), and $u(t), t \geq 0$, is the infusion rate of the anesthetic drug propofol into the central compartment. The transfer coefficients are assumed to be functions of the drug concentration c since it is well known that the pharmacokinetics of propofol are influenced by cardiac output [28] and, in turn, cardiac output is influenced by propofol plasma concentrations, both due to *venodilation* (pooling of blood in dilated vains) [29] and myocardial depression [30]. Finally, it is important to note that the compartmental model (38)–(40)

is already in the normal form basis (5)–(7), and hence, there is no need to construct a global diffeomorphism to transform (38)–(40) into the form of (5)–(7).

Experimental data indicate that the transfer coefficients $a_{ij}(\cdot)$ are nonincreasing functions of the propofol concentration [29], [30]. The most widely used empirical models for pharmacodynamic concentration-effect relationships are modifications of the Hill equation [31]. Applying this almost ubiquitous empirical model to the relationship between transfer coefficients implies that

$$a_{ij}(c) = A_{ij}Q_{ij}(c), \quad Q_{ij}(c) = \frac{Q_0 \mathrm{C}_{50,ij}^{\alpha_{ij}}}{(\mathrm{C}_{50,ij}^{\alpha_{ij}} + c^{\alpha_{ij}})}$$

where, for $i, j \in \{1,2,3\}$, $i \neq j$, $\mathrm{C}_{50,ij}$ is the drug concentration associated with a 50% decrease in the transfer coefficient, α_{ij} is a parameter that determines the steepness of the concentration-effect relationship, and A_{ij} are positive constants. Note that both pharmacokinetic parameters are functions of i and j, that is, there are distinct Hill equations for each transfer coefficient. Furthermore, since for many drugs the rate of metabolism $a_{11}(c)$ is proportional to the rate of transport of drug to the liver we assume that $a_{11}(c)$ is also proportional to the cardiac output so that $a_{11}(c) = A_{11}Q_{11}(c)$.

To illustrate the neuroadaptive control of propofol, we assume that $\mathrm{C}_{50,ij}$ and α_{ij} are independent of i and j. Also, since decreases in cardiac output are observed at clinically-utilized propofol concentrations we arbitrarily assign C_{50} a value of 4 $\mu\mathrm{g}/\mathrm{ml}$ since this value is in the mid-range of clinically utilized values. We also assign α a value of 3 [32]. This value is within the typical range of those observed for ligand-receptor binding (see the discussion in [33]). The nonnegative transfer and loss coefficients A_{12}, A_{21}, A_{13}, A_{31}, and A_{11}, and the parameters $\alpha > 1$, $\mathrm{C}_{50} > 0$, and $Q_0 > 0$, are uncertain due to patient gender, weight, pre-existing disease, age, and concomitant medication. Hence, the need for adaptive control to regulate intravenous anesthetics during surgery is essential.

Even though propofol concentration levels in the blood plasma will lead to the desired depth of anesthesia, they cannot be measured in real-time during surgery. Furthermore, we are more interested in drug *effect* (depth of hypnosis) rather than drug *concentration*. Hence, we consider a model involving pharmacokinetics (drug concentration as a function of time) and pharmacodynamics (drug effect as a function of concentration) for controlling consciousness. Specifically, we use an electroencephalogram (EEG) signal as a measure of hypnotic drug effect of anesthetic compounds on the brain [8], [34], [35]. Since electroencephalography provides real-time monitoring of the central nervous system activity, it can be used to quantify levels of consciousness, and hence, is amenable for feedback control in general anesthesia.

As discussed in the introduction, the BIS, an EEG indicator, has been proposed as a measure of hypnotic effect. This index quantifies the nonlinear relationships between the component frequencies in the electroencephalogram, as well as analyzing their phase and amplitude. The BIS signal is related to drug concentration by the empirical relationship

$$\mathrm{BIS}_n(c_{\mathrm{eff}}(t)) = \mathrm{BIS}_0 \left(1 - \frac{c_{\mathrm{eff}}^{\gamma}(t)}{c_{\mathrm{eff}}^{\gamma}(t) + \mathrm{EC}_{50}^{\gamma}}\right) + n(t) \quad (41)$$

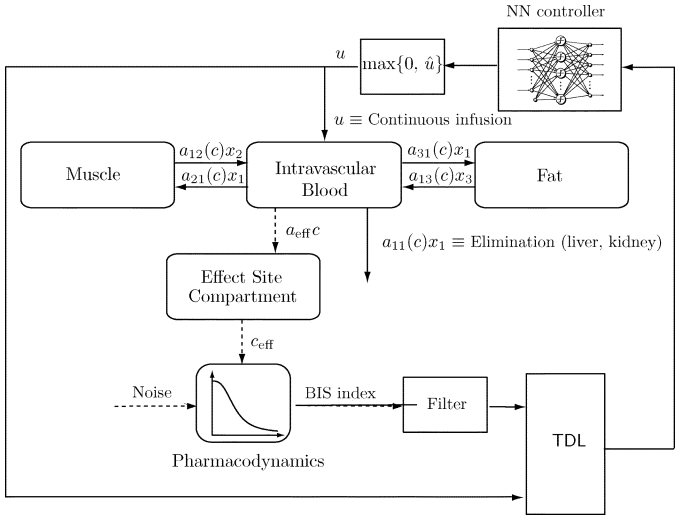

Fig. 3. Combined pharmacokinetic/pharmacodynamic control model.

where BIS_0 denotes the baseline (awake state) value and, by convention, is typically assigned a value of 100, c_{eff} is the propofol concentration in $\mu\mathrm{g}/\mathrm{ml}$ in the effect-site compartment (brain), EC_{50} is the concentration at half maximal effect and represents the patient's sensitivity to the drug, γ determines the degree of nonlinearity in (41), and n is a high-frequency observation noise signal. Here, the effect-site compartment is introduced to account for finite equilibration time between the central compartment concentration and the central nervous system concentration [36].

The effect-site compartment concentration is related to the concentration in the central compartment by the first-order model [36]

$$\dot{c}_{\mathrm{eff}}(t) = a_{\mathrm{eff}}(c(t) - c_{\mathrm{eff}}(t)), \quad c_{\mathrm{eff}}(0) = c(0), \quad t \geq 0 \quad (42)$$

where a_{eff} in min^{-1} is an unknown positive time constant. In reality, the effect-site compartment equilibrates with the central compartment in a matter of a few minutes. The parameters a_{eff}, EC_{50}, and γ are determined by data fitting and vary from patient to patient. BIS index values of 0 and 100 correspond, respectively, to an *isoelectric* EEG signal (no cerebral electrical activity) and an EEG signal of a fully conscious patient; the range between 40 and 60 indicates a moderate hypnotic state [34]. Fig. 3 shows the combined pharmacokinetic/pharmacodynamic control model for the distribution of propofol.

For set-point regulation define $e(t) \triangleq x(t) - x_e$, where $x_e \in \mathbb{R}_+^4$ is the set point satisfying the equilibrium condition for (38)–(40) and (42) with $x_1(t) \equiv x_{e1}$, $x_2(t) \equiv x_{e2}$, $x_3(t) \equiv x_{e3}$, $x_4(t) = c_{\mathrm{eff}}(t) \equiv \mathrm{EC}_{50}$, and $u(t) \equiv u_e$, so that $f_e(e) = [f_{e1}(e), f_{e2}(e), f_{e3}(e), f_{e4}(e)]^{\mathrm{T}}$ is given by

$$\begin{aligned}
f_{e1}(e) = &-[a_e(c) + a_{21}(c) + a_{31}(c)](e_1 + x_{e1}) \\
&+ a_{12}(c)(e_2 + x_{e2}) + a_{13}(c)(e_3 + x_{e3}) \\
&- [a_e(c_e) + a_{21}(c_e) + a_{31}(c_e)]x_{e1} \\
&+ a_{12}(c_e)x_{e2} + a_{13}(c_e)x_{e3}, \\
f_{e2}(e) = &\, a_{21}(c)(e_1 + x_{e1}) - a_{12}(c)(e_2 + x_{e2}) \\
&- [a_{21}(c_e)x_{e1} - a_{12}(c_e)x_{e2}], \\
f_{e3}(e) = &\, a_{31}(c)(e_1 + x_{e1}) - a_{13}(c)(e_3 + x_{e3}) \\
&- [a_{31}(c_e)x_{e1} - a_{13}(c_e)x_{e3}], \\
f_{e4}(e) = &\, a_{\mathrm{eff}}(c - (e_4 + \mathrm{EC}_{50})) - a_{\mathrm{eff}}(e_e - \mathrm{EC}_{50})
\end{aligned}$$

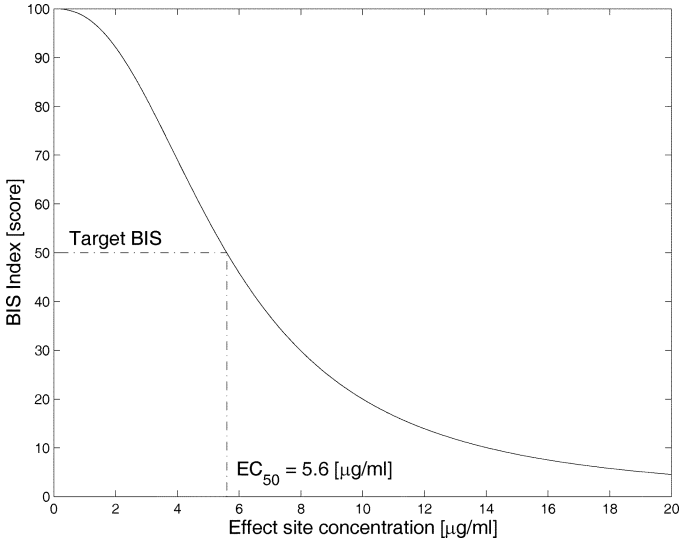

Fig. 4. BIS Index versus effect site concentration.

where $c_e \triangleq x_{e1}/V_{\rm c}$. The existence of this equilibrium point follows from the fact that the Jacobian of (38)–(40) and (42) is essentially nonnegative and every solution of (38)–(40) and (42) is bounded [37]. Next, linearizing $f_e(e)$ about 0 and computing the eigenvalues of the resulting Jacobian matrix, it can be shown that x_e is asymptotically stable. Hence, Assumption 3.1 is satisfied for our clinical model.

In the following simulation involving the infusion of the anesthetic drug propofol we set $\mathrm{EC}_{50} = 5.6\ \mu\mathrm{g/ml}$, $\gamma = 2.39$, and $\mathrm{BIS}_0 = 100$, so that the BIS signal is shown in Fig. 4. The target (desired) BIS value, $\mathrm{BIS}_{\rm target}$, is set at 50. Here, we use the neuroadaptive output feedback controller

$$u(t) = \max\{0, \hat{u}(t)\} \tag{43}$$

where

$$\hat{u}(t) = -\frac{\hat{W}_1^{\rm T}(t)\sigma_1(\zeta(t))}{\hat{b} + \hat{W}_2^{\rm T}(t)\sigma_2(\zeta(t))}$$
$$\zeta(t) = [\mathrm{BIS_f}(t-d), \mathrm{BIS_f}(t-2d), u(t-d), u(t-2d)]^{\rm T}$$

$\hat{b} > 0$, $d > 0$, with update laws

$$\dot{\hat{W}}_1(t) = Q_{\mathrm{BIS}_1}\mathrm{Proj}[\hat{W}_1(t), -\sigma_1(\zeta(t))\xi_{\rm c}^{\rm T}(t)\tilde{P}B_0] \quad \hat{W}_1(0) = \hat{W}_{10},\ t \geq 0$$
$$\dot{\hat{W}}_2(t) = Q_{\mathrm{BIS}_2}\mathrm{Proj}[\hat{W}_2(t), -\sigma_2(\zeta(t))u(t)\xi_{\rm c}^{\rm T}(t)\tilde{P}B_0] \quad \hat{W}_2(0) = \hat{W}_{20}$$

where Q_{BIS_1} and Q_{BIS_2} are positive constants and $\xi_{\rm c}(t) \in \mathbb{R}^2$, $t \geq 0$, is the solution to the estimator dynamics

$$\dot{\xi}_{\rm c}(t) = A\xi_{\rm c}(t) + L(\mathrm{BIS_f}(t) - y_{\rm c}(t) - \mathrm{BIS}_{\rm target}) \quad \xi_{\rm c}(0) = \xi_{\rm c0},\quad t \geq 0 \tag{44}$$
$$y_{\rm c}(t) = C\xi_{\rm c}(t) \tag{45}$$

where $A \in \mathbb{R}^{2\times 2}$, $L \in \mathbb{R}^{2\times 1}$, $C = [1,0]^{\rm T}$, and $\mathrm{BIS_f}(t)$ is output of the second-order, low-pass asymptotically stable filter

$$\dot{x}_{\rm f}(t) = A_{\rm f}x_{\rm f}(t) + B_{\rm f}\mathrm{BIS}_n(t),\ x_{\rm f}(0) = [\mathrm{BIS_f}(0), 0]^{\rm T},\quad t \geq 0 \tag{46}$$
$$\mathrm{BIS_f}(t) = C_{\rm f}x_{\rm f}(t) \tag{47}$$

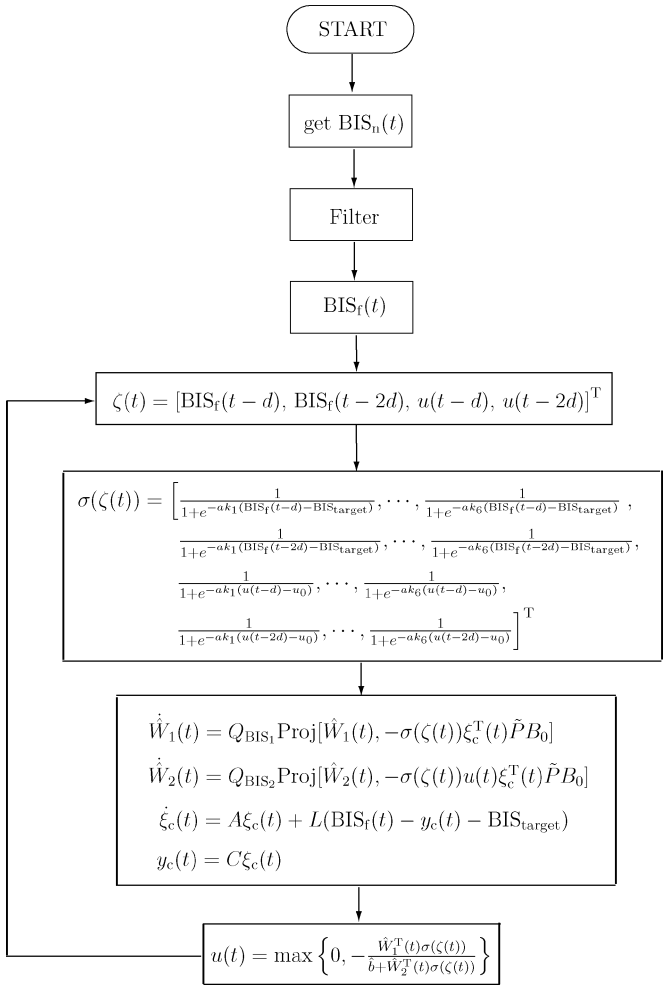

Fig. 5. Flowchart for the neuroadaptive control algorithm.

where

$$A_{\rm f} = \begin{bmatrix} 0 & 1 \\ -\omega_n^2 & -2\zeta\omega_n \end{bmatrix}$$

$B_{\rm f} = [0,\ \omega_n^2]^{\rm T}$, $C_{\rm f} = [1,0]^{\rm T}$, $\omega_n = 5$ rad/s, $\zeta = 0.7$, and $\mathrm{BIS_f}(0) = 100$. Here, we model $n(t)$ as a noise signal generated by a SIMULINK band-limited white noise block with a noise power parameter of 0.0001 amplified 100 times. Now, it follows from Theorem 3.1 that there exist positive constants ε and T such that $|\mathrm{BIS}(t) - \mathrm{BIS}_{\rm target}| \leq \varepsilon, t \geq T$, where $\mathrm{BIS}(t)$ is given by (41) with $n(t) \equiv 0$, for all nonnegative values of the pharmacokinetic transfer and loss coefficients $A_{12}, A_{21}, A_{13}, A_{31}, A_{11}$ as well as all nonnegative coefficients α, C_{50}, and Q_0. A flowchart for the neuroadaptive control algorithm is shown in Fig. 5.

For our simulation, we assume $V_{\rm c} = (0.228\ \mathrm{l/kg})(M\ \mathrm{kg})$, where $M = 70$ kg is the mass of the patient, $A_{21}Q_0 = 0.112\ \mathrm{min}^{-1}$, $A_{12}Q_0 = 0.055\ \mathrm{min}^{-1}$, $A_{31}Q_0 = 0.0419\ \mathrm{min}^{-1}$, $A_{13}Q_0 = 0.0033\ \mathrm{min}^{-1}$, $A_eQ_0 = 0.119\ \mathrm{min}^{-1}$, $a_{\rm eff} = 3.4657\ \mathrm{min}^{-1}$, $\alpha = 3$, and $\mathrm{C}_{50} = 4\ \mu$g/ml [27], [32]. Note that the parameter values for α and C_{50} probably exaggerate the effect of propofol on cardiac output. They have been selected to accentuate nonlinearity but they are not biologically unrealistic. Furthermore, to illustrate the proposed neuroadaptive controller we switch the pharmacodynamic parameters EC_{50} and γ, respectively, from 5.6 μg/ml and 2.39 to 7.2 μg/ml and 3.39 at $t = 15$ min and back to 5.6 μg/ml and 2.39 at $t = 30$ min.

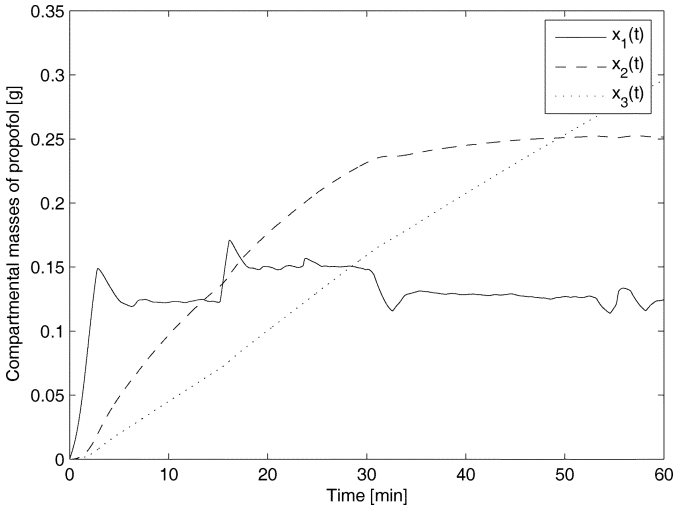

Fig. 6. Compartmental masses versus time.

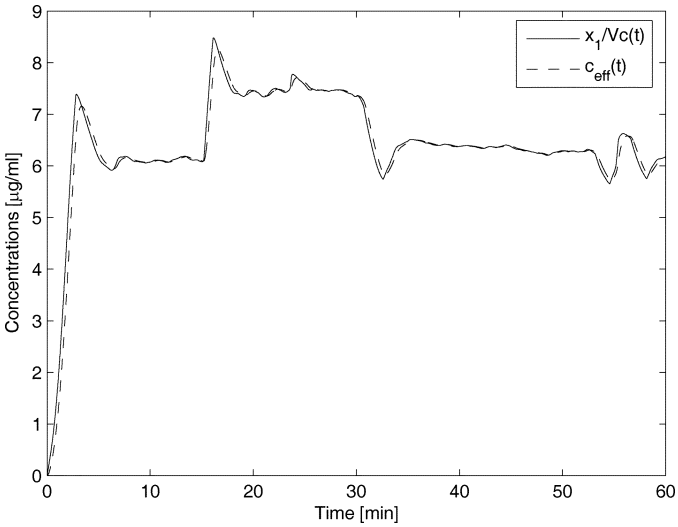

Fig. 7. Concentrations in central and effect site compartments versus time.

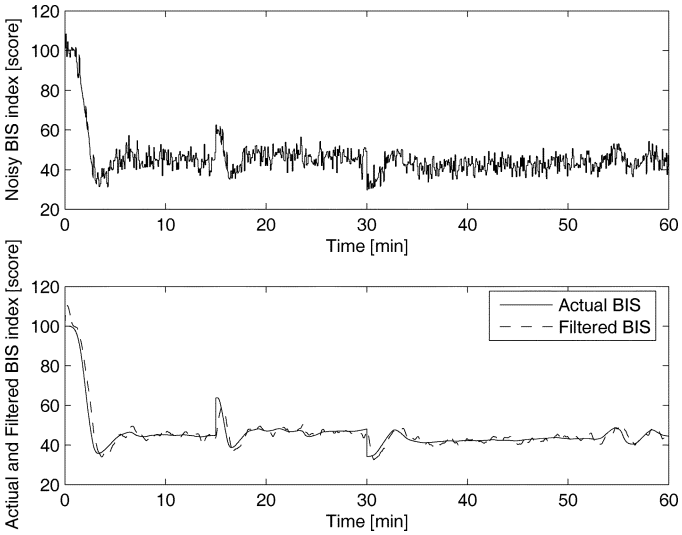

Fig. 8. BIS signal versus time.

Here, we consider noncardiac surgery since cardiac surgery often utilizes hypothermia which itself changes the BIS signal.

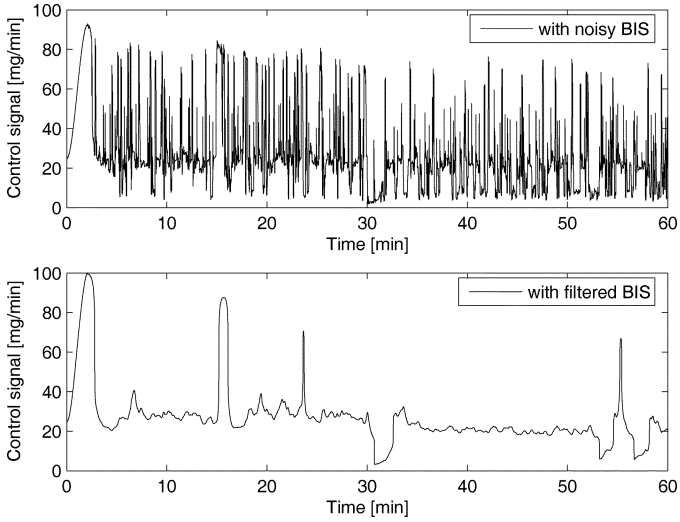

Fig. 9. Control signal (infusion rate) versus time.

With

$$A = \begin{bmatrix} 0 & 1 \\ -1 & -1 \end{bmatrix}$$

$L = [0,1]^{\mathrm{T}}$, $\hat{b} = 1$, $Q_{\mathrm{BIS}_1} = 2.0 \times 10^{-4}$ g/min^2, $Q_{\mathrm{BIS}_2} = 4.0 \times 10^{-4}$ g/min^2, $d = 0.005$, and initial conditions $x_1(0) = x_2(0) = x_3(0) = 0$ g, $c_{\mathrm{eff}}(0) = 0$ g/ml, $\xi_{\mathrm{c}}(0) = [0, 0]^{\mathrm{T}}$, $\hat{W}_1(0) = 1 \times 10^{-3}[-3_{12\times1}, 1_{12\times1}]^{\mathrm{T}}$, $\hat{W}_2(0) = 0_{24\times1}$, Fig. 6 shows the masses of propofol in the three compartments versus time. Fig. 7 shows the concentrations in the central and effect-site compartments versus time. Note that the effect-site compartment equilibrates with the central compartment in a matter of a few minutes. Fig. 8 shows the noisy, actual, and filtered controlled BIS signals versus time. Finally, Fig. 9 shows the control signal (propofol infusion rate) versus time predicated on the actual and filtered BIS signal.

For our simulation we used

$$\begin{aligned}
&\sigma_1(\zeta(t)) \\
&\quad = \sigma_2(\zeta(t)) = \Bigg[\frac{1}{1+e^{-ak_1(\mathrm{BIS_f}(t-d)-\mathrm{BIS_{target}})}}, \\
&\qquad \cdots, \frac{1}{1+e^{-ak_6(\mathrm{BIS_f}(t-d)-\mathrm{BIS_{target}})}}, \\
&\qquad \cdots, \frac{1}{1+e^{-ak_1(\mathrm{BIS_f}(t-2d)-\mathrm{BIS_{target}})}}, \\
&\qquad \cdots, \frac{1}{1+e^{-ak_6(\mathrm{BIS_f}(t-2d)-\mathrm{BIS_{target}})}}, \\
&\qquad \cdots, \frac{1}{1+e^{-ak_1(u(t-d)-u_0)}}, \\
&\qquad \cdots, \frac{1}{1+e^{-ak_6(u(t-d)-u_0)}}, \\
&\qquad \cdots, \frac{1}{1+e^{-ak_1(u(t-2d)-u_0)}}, \\
&\qquad \cdots, \frac{1}{1+e^{-ak_6(u(t-2d)-u_0)}} \Bigg]^{\mathrm{T}}
\end{aligned}$$

where $s_1 = s_2 = 24$, $a = 0.1$, $k_1 = 1$, $k_2 = 2$, $k_3 = 6$, $k_4 = 24$, $k_5 = 120$, $k_6 = 720$, and $u_0 = 15$ mg/min. Even though we

did not calculate the analytical bounds given by (33) due to the fact that one has to solve an optimization problem with respect to (14) and (15) to obtain ε_i^* and $w_{i\max}^*$, $i = 1, 2$, the closed-loop BIS signal response shown in Fig. 8 is clearly acceptable. Furthermore, the basis functions for $\sigma_i(\zeta)$, $i = 1, 2$, are chosen to cover the domain of interest of our pharmacokinetic/pharmacodynamic problem since we know that the BIS index varies from 0 to 100. Hence, the basis functions are distributed over that domain. The number of basis functions, however, is based on trial and error. This goes back to the Stone–Weierstrass theorem which only provides an existence result without any constructive guidelines. Finally, we note that simulations using a larger number of neurons resulted in imperceptible differences in the closed-loop system performance.

The neuroadaptive control algorithm (43)–(45) does not require knowledge of the pharmacokinetic and pharmacodynamic parameters, in contrast to previous algorithms for closed-loop control of anesthesia [38], [39]. However, the neuroadaptive controller (43)–(45) does not account for time delays due to the proprietary signal-averaging algorithm within the BIS monitor. Given the clinical observation that there is often a substantial delay between observed changes in patient status and a change in the BIS signal, other measures of depth of anesthesia may be needed [40].

V. Clinical Evaluation Trials

We have performed 15 clinical trials with the neuroadaptive controller (43)–(45) at the Northeast Georgia Medical Center, Gainesville, GA. In initial clinical testing, we implemented (43)–(45) using a Dell Latitude C610 laptop computer with a Pentium (R) III processor running under Windows XP, an Aspect A 2000 BIS monitor (rev 3.23), and a Harvard PHD 2000 programmable research pump. The BIS monitor sends a data stream, which is updated every 5 s. This data stream contains the BIS signal as well as other parameters such as date, time, signal quality indicator, raw EEG information, and electromyographic data. The data are sent to the serial port of the laptop computer.

The infusion rate $u(t)$ for the controller is calculated by employing a forward Euler method to update the neural network weights $\hat{W}_1(t)$ and $\hat{W}_2(t)$ every 0.5 s, using the BIS signal. The infusion rate is communicated to the infusion pump using a 9600 bpm, 8 data bits, 2 stop bits, and zero parity protocol with the aid of a USB-serial port adaptor. An updated infusion rate is sent to the pump every 1 sec. Pharmacokinetic simulations predict that a pump update every 5 s or less is adequate in the context of the algorithm under evaluation. An update interval of 1 s was selected in anticipation that future algorithms might benefit from the faster update rate. In order to filter the noisy BIS signal we used a second-order, low-pass filter with natural frequency $\omega_n = 0.01$ rad/s and damping ratio $\zeta = 0.707$.

The neuroadaptive control algorithm was programmed in Java, an object-oriented programming language chosen for its multiplatform portability tools for rapid prototyping. The program is organized into five modules, namely, bisloader, bislogger, controller, pumplogger, and pumploader. Bisloader and bislogger handle communication between the BIS monitor and the computer, while pumploader and pumplogger manage the Harvard pump apparatus. The module bisloader finds the serial port that receives the BIS signal by using the Java class CommPort Identifier, and then invokes bislogger. Bislogger uses the Java class SerialPort EventListener to read the signal, and uses the class StringTokenizer to parse the BIS signal from the input stream. The infusion rate is calculated by the controller module. Finally, pumploader opens the serial port communicating to the pump and establishes the communication protocol, while pumplogger delivers the infusion rate to the pump.

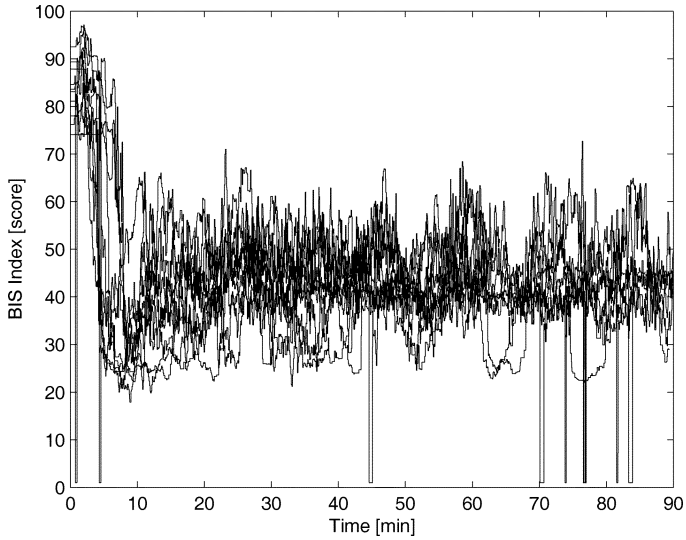

Fig. 10. Controlled BIS signal versus time for 10 patients.

The protocol for clinical evaluation of the system was approved by the Institutional Review Board of Northeast Georgia Medical Center. Patients are enrolled after giving informed consent. Our protocol excludes patients requiring emergency surgery, pediatric patients, hemodynamically unstable patients, and patients for whom we anticipate difficult airway management. Otherwise, all elective surgical patients who can provide informed consent are candidates. Preoperative management, including administration of anti-anxiolytic drugs, is left to the discretion of the attending anesthesiologist. Propofol is delivered using the BIS-computer-pump system with a target value of 50. In addition to propofol, all patients receive infusions of either sufentanil or fentanyl with loading doses of 0.25 or 2μg/ml and continuous infusions of 0.25 or 2 $(\mu\text{g/ml})/\text{hr}$, respectively, to provide analgesia. To ensure patient safety, an independent anesthesia provider observes the progress of the study and can terminate the study if it appears that the patient's safety is being jeopardized by either overdosing or underdosing of propofol.

VI. Results and Discussion

Patient demographics (for 10 patients) are presented in Table I. The median BIS value after induction was 43. Four of the ten patients required phenylephrine to treat hypotension during induction (average dose 1075 μg with a standard deviation of 809.8 μg). The actual and filtered BIS signals versus time and control signal (propofol infusion rate) versus time for 10 patients are shown in Figs. 10–12. The effect of using the actual (i.e., noisy) versus filtered BIS signal to generate

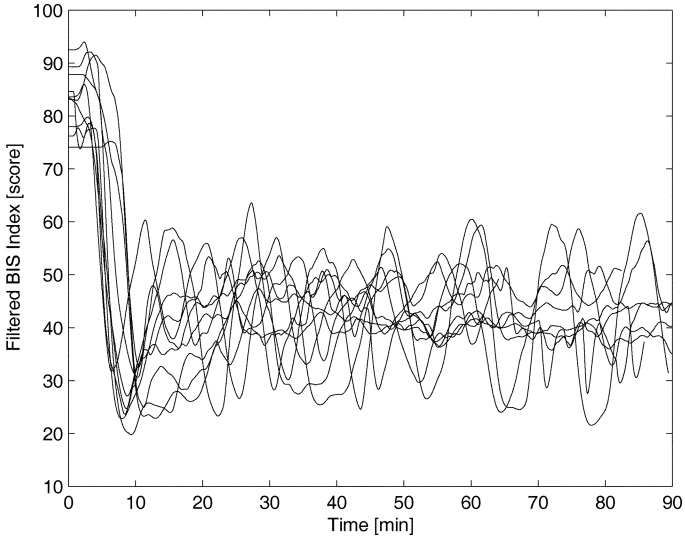

Fig. 11. Filtered BIS signal versus time for 10 patients.

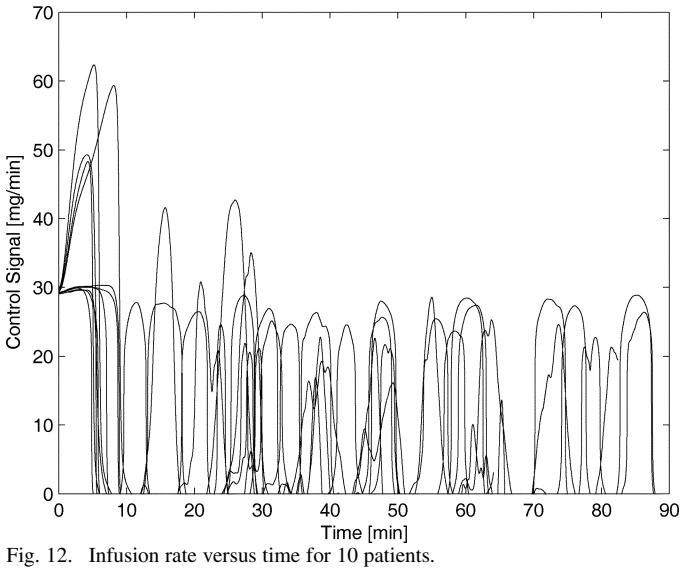

Fig. 12. Infusion rate versus time for 10 patients.

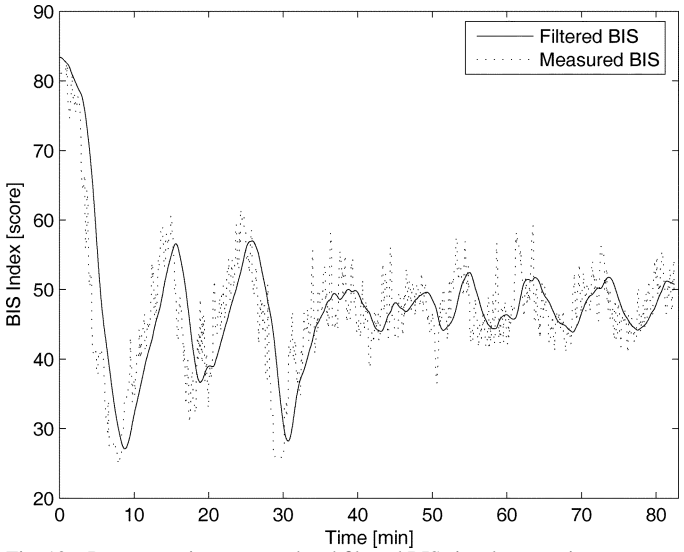

Fig. 13. Representative measured and filtered BIS signal versus time.

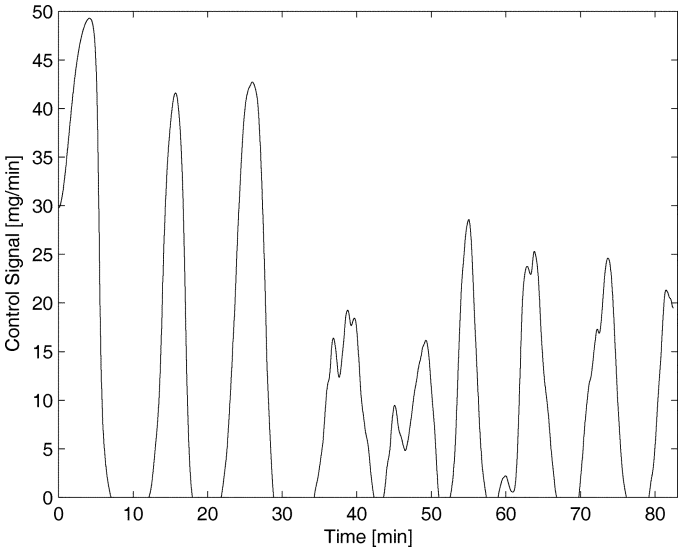

Fig. 14. Representative infusion rate predicated on filtered BIS signal versus time.

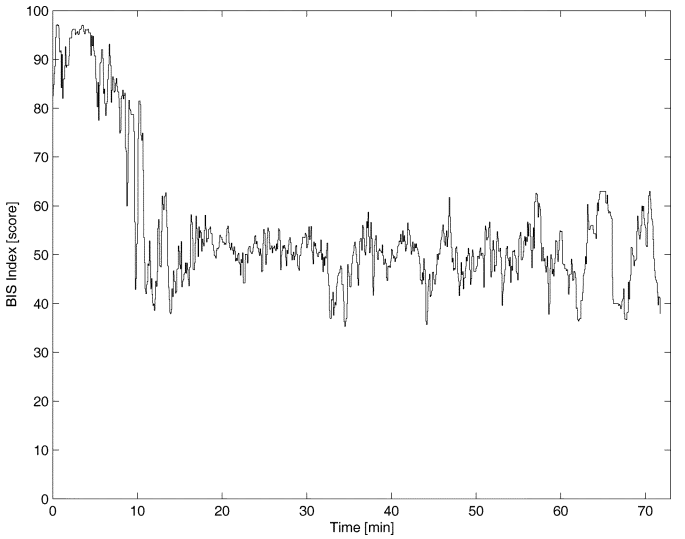

Fig. 15. Representative measured (noisy) BIS signal versus time.

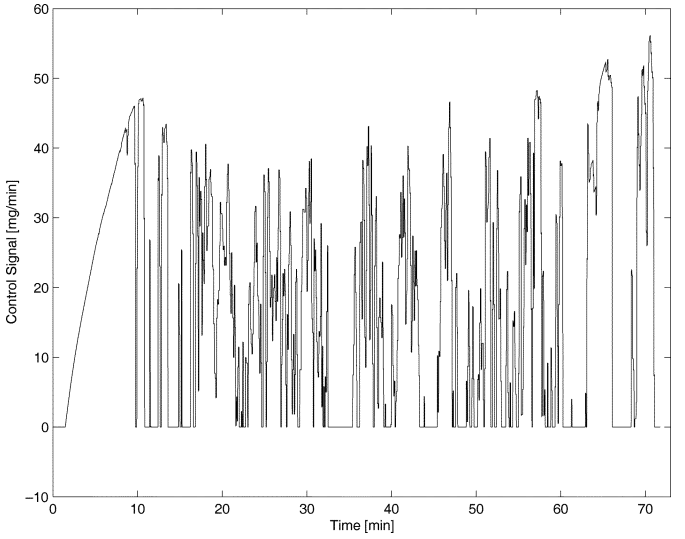

Fig. 16. Representative infusion rate predicated on measured (noisy) BIS signal versus time.

the control signal is illustrated in Figs. 13–16. In particular, Fig. 14 shows the control signal predicated on the filtered BIS signal shown in Fig. 13, whereas Fig. 16 shows control signal predicated on the actual (i.e., noisy) BIS signal shown in Fig. 15. Several performance measures of the control algorithm

TABLE I
DEMOGRAPHICS OF NEUROADAPTIVE CONTROL ALGORITHM

Age	59.0 years (18.0)
Weight	91.8 kg (23.3)
Gender	8 M / 2 F
Procedure	8 CABG †, 1 Thoracoscopy, 1 AVR ‡

* All values are mean with standard deviation in parentheses.
† CABG is Coronary Artery Bypass Grafting.
‡ AVR is Aortic Valve Replacement.

TABLE II
BIS, BIAS AND MAPE OF NEUROADAPTIVE CONTROL ALGORITHM

No	median BIS	Bias(%)	MAPE(%)
1	41.2	-17.6	20.1
2	41.2	-17.6	18.8
3	42.2	-15.8	17.4
4	46.5	-7.1	12.4
5	46.0	-8.0	20.4
6	42.7	-14.6	17.2
7	47.2	-5.5	8.1
8	41.1	-17.8	22.3
9	41.9	-16.3	17.0
10	39.5	-21.1	23.1

TABLE III
OVERSHOOT, OUTSIDE TIME OF NEUROADAPTIVE CONTROL ALGORITHM

No	Overshoot	Outside Time (%)
1	23.3	27.7
2	22.8	23.0
3	24.7	15.2
4	31.8	18.0
5	30.6	42.2
6	32.6	14.6
7	27.1	12.9
8	19.8	37.8
9	23.7	13.4
10	24.9	36.3

such as median BIS, bias (the median of measured BIS minus target, normalized to the target), the median absolute value of the performance error (MAPE) (with performance error defined as measured BIS minus the target, normalized to the target) are summarized in Table II. We observed that with induction all patients had some "overshoot" of the target BIS of 50, that is, a BIS value less than 50. In Table III we present, overshoot, and outside time (the percentage of study time that the individual patients had BIS values outside of the 35–60 range).

As noted in the introduction and [15], several other systems for closed-loop control of intravenous anesthesia have been previously described. The most direct comparison is to the results of Struys *et al.* [39]. The median absolute performance error of their controller was 7.7% in comparison to our 17.7%. The fraction of time that patients in the Struys *et al.* study were outside a BIS range of 35–60 was 11% compared to our 20.5%. Based on these measures, one would surmise that the clinical performance of the controller described by Struys *et al.* is superior. However, there are several factors that make direct comparisons tenuous. First, study designs were quite different. Struys *et al.* supplemented propofol with a continuous infusion of remifentanil while we used a bolus then continuous infusion of sufentanil. The rapid kinetics of remifentanil in comparison to sufentanil implies that opioid levels were more constant over time in the Struys *et al.* study than in ours. A constant opioid concentration could be expected to more effectively blunt arousal responses in the BIS with surgical stimulation. And, as noted by Glass and Rampil in the editorial accompanying the publication by Struys *et al.*; the remifentanil dose used by Struys *et al.* is sufficient to blunt responses to surgical stimulation and reduce the propofol concentration to that needed to prevent consciousness [41].

Another key difference in study protocols is that Struys *et al.* initiated propofol administration with open-loop control and did not "close" the loop until the BIS reached 50. The controllers evaluated in this study were used for the induction as well as the maintenance of anesthesia. Finally, we note that model-based controllers may be expected to perform better than model-independent controllers as long as the model is correct. The three compartment mammillary pharmacokinetic model and the modified Hill equation pharmacodynamic model are well established and they could be expected to facilitate closed-loop control in the "average" patient who conforms to the models. However, model-based controllers could fail in patients who do not conform to the model and the studies done of closed-loop anesthesia to date do not have sufficient numbers to evaluate failure due to model nonconformance. Furthermore, we know that the three compartment mammilary model is not accurate when the propofol concentration is increased acutely, as occurs during induction and when surgical arousal is not blunted by opioids. Thus, we believe that comparison of controllers will not be definitive until larger numbers of patients are studied, so that one might encounter outlier patients, and with more demanding anesthetic/surgical conditions requiring wider ranges of anesthetic concentrations.

APPENDIX
PROOF OF THEOREM 3.1

In this appendix, we prove Theorem 3.1. First, define

$$\hat{W}_{1\mathrm{u}}(t) \triangleq \begin{cases} \hat{W}_1(t), & \text{if } \hat{u}(t) \geq\geq 0 \\ 0, & \text{otherwise.} \end{cases} \tag{48}$$

Next, defining $e_\xi(t) \triangleq \xi(t) - \xi_e$, $e_z(t) \triangleq z(t) - z_e$, $\tilde{\xi}(t) \triangleq \xi_{\mathrm{c}}(t) - e_\xi(t)$, and $\tilde{x}_{\mathrm{f}}(t) \triangleq x_{\mathrm{f}}(t) - x_{\mathrm{f}_e}$, and using (5)–(12), (14), (15), and (25) it follows from (5), (6), (30), and (16)–(19) that

$$\begin{aligned}
\dot{e}_\xi(t) &= Ae_\xi(t) + A\xi_e + \tilde{f}_{\mathrm{u}}(\xi(t), z(t)) + G_\xi(\xi(t), z(t))u(t) \\
&= Ae_\xi(t) + B_0\hat{G}(\mathcal{T}(x(t)))u(t) \\
&\quad + B_0[f_{\mathrm{u}}(\mathcal{T}(x(t))) - f_{\mathrm{u}}(\mathcal{T}(x_e)) - \hat{G}(\mathcal{T}(x_e))u_e] \\
&\quad + B_0\left(\hat{B} + \hat{W}_2^{\mathrm{T}}(t)[I_m \otimes \sigma_2(\zeta(t))]\right)\Big(-u(t) \\
&\quad - \left(\hat{B} + \hat{W}_2^{\mathrm{T}}(t)[I_m \otimes \sigma_2(\zeta(t))]\right)^{-1} \\
&\quad \cdot \hat{W}_{1\mathrm{u}}^{\mathrm{T}}(t)\sigma_1(\zeta(t))\Big) \\
&= Ae_\xi(t) + B_0[W_1^{\mathrm{T}}\hat{\sigma}_1(x(t)) + \varepsilon_1(x(t))] \\
&\quad + B_0\left(W_2^{\mathrm{T}}[I_m \otimes \hat{\sigma}_2(x(t))] + \varepsilon_2(x(t))\right)u(t) \\
&\quad - B_0\hat{W}_2^{\mathrm{T}}(t)[I_m \otimes \sigma_2(\zeta(t))]u(t) \\
&\quad - B_0\hat{W}_{1\mathrm{u}}^{\mathrm{T}}(t)\sigma_1(\zeta(t)) \\
&= Ae_\xi(t) + B_0[W_1^{\mathrm{T}}\hat{\sigma}_1(x(t)) - W_1^{\mathrm{T}}\sigma_1(\zeta(t)) \\
&\quad + W_1^{\mathrm{T}}\sigma_1(\zeta(t)) + \varepsilon_1(x(t))] \\
&\quad + B_0(W_2^{\mathrm{T}}[I_m \otimes \hat{\sigma}_2(x(t))] - W_2^{\mathrm{T}}[I_m \otimes \sigma_2(\zeta(t))]
\end{aligned}$$

$$
\begin{aligned}
&+ W_2^{\mathrm{T}}[I_m \otimes \sigma_2(\zeta(t))] + \varepsilon_2(x(t)))u(t)\\
&- B_0\hat{W}_2^{\mathrm{T}}(t)[I_m \otimes \sigma_2(\zeta(t))]u(t)\\
&- B_0\hat{W}_{1\mathrm{u}}^{\mathrm{T}}(t)\sigma_1(\zeta(t))\\
=\ & Ae_\xi(t) - B_0\tilde{W}_1^{\mathrm{T}}(t)\sigma_1(\zeta(t))\\
&- B_0\tilde{W}_2^{\mathrm{T}}(t)[I_m \otimes \sigma_2(\zeta(t))]u(t)\\
&+ B_0(\hat{W}_1(t) - \hat{W}_{1\mathrm{u}}(t))^{\mathrm{T}}\sigma_1(\zeta(t)) + B_0\varepsilon_1(x(t))\\
&+ B_0\varepsilon_2(x(t))u(t) + B_0W_1^{\mathrm{T}}[\hat{\sigma}_1(x(t)) - \sigma_1(\zeta(t))]\\
&+ B_0W_2^{\mathrm{T}}\left[I_m \otimes (\hat{\sigma}_2(x(t)) - \sigma_2(\zeta(t)))\right]u(t),\\
&\qquad e_\xi(0) = \xi_0 - \xi_e, \quad t \geq 0, \qquad (49)\\
\dot{e}_z(t) =\ & \tilde{f}_z(e_\xi(t), e_z(t)), \quad e_z(0) = z_0 - z_e \qquad (50)\\
\dot{\tilde{\xi}}(t) =\ & \dot{\xi}_{\mathrm{c}}(t) - \dot{e}_\xi(t)\\
=\ & \tilde{A}\tilde{\xi}(t) + B_0\tilde{W}_1^{\mathrm{T}}(t)\sigma_1(\zeta(t))\\
&+ B_0\tilde{W}_2^{\mathrm{T}}(t)[I_m \otimes \sigma_2(\zeta(t))]u(t)\\
&- B_0(\hat{W}_1(t) - \hat{W}_{1\mathrm{u}}(t))^{\mathrm{T}}\sigma_1(\zeta(t)) - B_0\varepsilon_1(x(t))\\
&+ B_0\varepsilon_2(x(t))u(t) - B_0W_1^{\mathrm{T}}[\hat{\sigma}_1(x(t)) - \sigma_1(\zeta(t))]\\
&- B_0W_2^{\mathrm{T}}\left[I_m \otimes (\hat{\sigma}_2(x(t)) - \sigma_2(\zeta(t)))\right]u(t)\\
&+ LC_{\mathrm{f}}\tilde{x}_{\mathrm{f}}(t) - LCe_\xi(t), \ \tilde{\xi}(0) = \xi_{\mathrm{c}0} - \xi_0 + \xi_e \qquad (51)
\end{aligned}
$$

where $\tilde{A} \triangleq A - LC$, $\tilde{f}_z(e_\xi, e_z) \triangleq f_z(e_\xi + x_e, e_z + z_e)$, $\tilde{W}_i(t) \triangleq \hat{W}_i(t) - W_i$, $i = 1, 2$, and $\hat{\sigma}_1 : \mathbb{R}^n \to \mathbb{R}^{s_1}$ and $\hat{\sigma}_2 : \mathbb{R}^n \to \mathbb{R}^{s_2}$ are such that each component of $\hat{\sigma}_1(\cdot)$ and $\hat{\sigma}_2(\cdot)$ takes values between 0 and 1.

To show ultimate boundedness of the closed-loop system (27), (28), (49)–(51), consider the Lyapunov-like function

$$
\begin{aligned}
V(e_\xi, e_z, \tilde{\xi}, \tilde{W}_1, \tilde{W}_2, \tilde{x}_{\mathrm{f}}) = {} & e_\xi^{\mathrm{T}}Pe_\xi + \tilde{\xi}^{\mathrm{T}}\tilde{P}\tilde{\xi} + \mathrm{tr}\,\tilde{W}_1Q_1^{-1}\tilde{W}_1^{\mathrm{T}}\\
& + \mathrm{tr}\,\tilde{W}_2Q_2^{-1}\tilde{W}_2^{\mathrm{T}} + \tilde{x}_{\mathrm{f}}^{\mathrm{T}}\hat{P}\tilde{x}_{\mathrm{f}} \qquad (52)
\end{aligned}
$$

where $P > 0$, $\tilde{P} > 0$, and $\hat{P}$ satisfy (29), (32), and (20), respectively. Note that (52) satisfies $\alpha(\|x_1\|) \leq V(x_1, x_2) \leq \beta(\|x_1\|)$ with $x_1 = [e_\xi^{\mathrm{T}}, \tilde{\xi}^{\mathrm{T}}, (\mathrm{vec}\,\hat{W}_1)^{\mathrm{T}}, (\mathrm{vec}\,\hat{W}_2)^{\mathrm{T}}, \tilde{x}_{\mathrm{f}}^{\mathrm{T}}]^{\mathrm{T}}$, $x_2 = e_z$, $\alpha(\|x_1\|) = \beta(\|x_1\|) = \|x_1\|^2$, where

$$
\begin{aligned}
&\|x_1\|^2\\
&\triangleq e_\xi^{\mathrm{T}}Pe_\xi + \tilde{\xi}^{\mathrm{T}}\tilde{P}\tilde{\xi} + \mathrm{tr}\,\tilde{W}_1Q_1^{-1}\tilde{W}_1^{\mathrm{T}} + \mathrm{tr}\,\tilde{W}_2Q_2^{-1}\tilde{W}_2^{\mathrm{T}} + \tilde{x}_{\mathrm{f}}^{\mathrm{T}}\hat{P}\tilde{x}_{\mathrm{f}}
\end{aligned}
$$

and $\mathrm{vec}(\cdot)$ denotes the column stacking operator. Furthermore, $\alpha(\|x_1\|)$ is a class $\mathcal{K}_\infty$ function. Using (18), (19) and (4), the filter dynamics given by (16) and (17) can be rewritten as

$$
\begin{aligned}
&\dot{\tilde{x}}_{\mathrm{f}}(t) = A_{\mathrm{f}}\tilde{x}_{\mathrm{f}}(t) + B_{\mathrm{f}}(y(t) + n(t) - y_{\mathrm{d}}), \ \tilde{x}_{\mathrm{f}}(0) = x_{\mathrm{f}_0} - x_{\mathrm{f}_e},\\
&\qquad t \geq 0 \qquad (53)\\
&y_{\mathrm{f}}(t) = C_{\mathrm{f}}\tilde{x}_{\mathrm{f}}(t) + y_{\mathrm{d}}. \qquad (54)
\end{aligned}
$$

Now, letting $e_\xi(t)$, $\xi_{\mathrm{c}}(t)$, and $\tilde{x}_{\mathrm{f}}(t)$, $t \geq 0$, denote the solution to (49), (30), and (53), respectively, and using (14), (15), (22), (27), and (28), it follows that the time derivative of $V(e_\xi, e_z, \tilde{\xi}, \tilde{W}_1, \tilde{W}_2, \tilde{x}_{\mathrm{f}})$ along the closed-loop system trajectories is given by

$$
\begin{aligned}
&\dot{V}(e_\xi(t), e_z(t), \tilde{\xi}(t), \tilde{W}_1(t), \tilde{W}_2(t), \tilde{x}_{\mathrm{f}}(t))\\
&= 2e_\xi^{\mathrm{T}}(t)P\Big[Ae_\xi(t) - B_0\tilde{W}_1^{\mathrm{T}}(t)\sigma_1(\zeta(t))\\
&\quad - B_0\tilde{W}_2^{\mathrm{T}}(t)[I_m \otimes \sigma_2(\zeta(t))]u(t)\\
&\quad + B_0(\hat{W}_1(t) - \hat{W}_{1\mathrm{u}}(t))^{\mathrm{T}}\sigma_1(\zeta(t))\\
&\quad + B_0\varepsilon_1(x(t)) + B_0\varepsilon_2(x(t))u(t)\\
&\quad + B_0W_1^{\mathrm{T}}[\hat{\sigma}_1(x(t)) - \sigma_1(\zeta(t))]\\
&\quad + B_0W_2^{\mathrm{T}}\left[I_m \otimes (\hat{\sigma}_2(x(t)) - \sigma_2(\zeta(t)))\right]u(t)\Big]\\
&\quad + 2\tilde{\xi}^{\mathrm{T}}(t)\tilde{P}\Big[\tilde{A}\tilde{\xi}(t) + B_0\tilde{W}_1^{\mathrm{T}}(t)\sigma_1(\zeta(t))\\
&\quad + B_0\tilde{W}_2^{\mathrm{T}}(t)[I_m \otimes \sigma_2(\zeta(t))]u(t)\\
&\quad - B_0(\hat{W}_1(t) - \hat{W}_{1\mathrm{u}}(t))^{\mathrm{T}}\sigma_1(\zeta(t)) - B_0\varepsilon_1(x(t))\\
&\quad + B_0\varepsilon_2(x(t))u(t) - B_0W_1^{\mathrm{T}}[\hat{\sigma}_1(x(t)) - \sigma_1(\zeta(t))]\\
&\quad - B_0W_2^{\mathrm{T}}\left[I_m \otimes (\hat{\sigma}_2(x(t)) - \sigma_2(\zeta(t)))\right]u(t)\Big]\\
&\quad + 2\,\mathrm{tr}\,\tilde{W}_1^{\mathrm{T}}(t)Q_1^{-1}\dot{\hat{W}}_1(t) + 2\,\mathrm{tr}\,\tilde{W}_2^{\mathrm{T}}(t)Q_2^{-1}\dot{\hat{W}}_2(t)\\
&\quad + 2\tilde{x}_{\mathrm{f}}^{\mathrm{T}}(t)\hat{P}\Big[A_{\mathrm{f}}\tilde{x}_{\mathrm{f}}(t) + B_{\mathrm{f}}(y(t) + n(t) - y_{\mathrm{d}})\Big]\\
&= -e_\xi^{\mathrm{T}}(t)Re_\xi(t) - \tilde{\xi}^{\mathrm{T}}(t)\tilde{R}\tilde{\xi}(t) - \tilde{x}_{\mathrm{f}}^{\mathrm{T}}(t)\hat{R}\tilde{x}_{\mathrm{f}}(t)\\
&\quad - 2e_\xi^{\mathrm{T}}(t)PB_0\tilde{W}_1^{\mathrm{T}}(t)\sigma_1(\zeta(t))\\
&\quad - 2e_\xi^{\mathrm{T}}(t)PB_0\tilde{W}_2^{\mathrm{T}}(t)[I_m \otimes \sigma_2(\zeta(t))]u(t)\\
&\quad + 2e_\xi^{\mathrm{T}}(t)PB_0(\hat{W}_1(t) - \hat{W}_{1\mathrm{u}}(t))^{\mathrm{T}}\sigma_1(\zeta(t))\\
&\quad + 2e_\xi^{\mathrm{T}}(t)PB_0(\varepsilon_1(x(t)) + \varepsilon_2(x(t))u(t))\\
&\quad + 2e_\xi^{\mathrm{T}}(t)PB_0(W_1^{\mathrm{T}}[\hat{\sigma}_1(x(t)) - \sigma_1(\zeta(t))]\\
&\quad + W_2^{\mathrm{T}}\left[I_m \otimes (\hat{\sigma}_2(x(t)) - \sigma_2(\zeta(t)))\right]u(t))\\
&\quad + 2\tilde{\xi}^{\mathrm{T}}(t)\tilde{P}B_0\tilde{W}_1^{\mathrm{T}}(t)\sigma_1(\zeta(t))\\
&\quad + 2\tilde{\xi}^{\mathrm{T}}(t)\tilde{P}B_0\tilde{W}_2^{\mathrm{T}}(t)[I_m \otimes \sigma_2(\zeta(t))]u(t)\\
&\quad - 2\tilde{\xi}^{\mathrm{T}}(t)\tilde{P}B_0(\hat{W}_1(t) - \hat{W}_{1\mathrm{u}}(t))^{\mathrm{T}}\sigma_1(\zeta(t))\\
&\quad - 2\tilde{\xi}^{\mathrm{T}}(t)\tilde{P}B_0(\varepsilon_1(x(t)) + \varepsilon_2(x(t))u(t))\\
&\quad - 2\tilde{\xi}^{\mathrm{T}}(t)\tilde{P}B_0(W_1^{\mathrm{T}}[\hat{\sigma}_1(x(t)) - \sigma_1(\zeta(t))]\\
&\quad + W_2^{\mathrm{T}}\left[I_m \otimes (\hat{\sigma}_2(x(t)) - \sigma_2(\zeta(t)))\right]u(t))\\
&\quad + 2\,\mathrm{tr}\,\tilde{W}_1^{\mathrm{T}}(t)\mathrm{Proj}(\hat{W}_1(t), -\sigma_1(\zeta(t))\xi_{\mathrm{c}}^{\mathrm{T}}(t)\tilde{P}B_0)\\
&\quad + 2\,\mathrm{tr}\,\tilde{W}_2^{\mathrm{T}}(t)\\
&\quad \cdot \mathrm{Proj}(\hat{W}_2(t), -[I_m \otimes \sigma_2(\zeta(t))]u(t)\xi_{\mathrm{c}}^{\mathrm{T}}(t)\tilde{P}B_0)\\
&\quad + 2\tilde{x}_{\mathrm{f}}^{\mathrm{T}}\hat{P}B_{\mathrm{f}}Ce_\xi(t) + 2\tilde{x}_{\mathrm{f}}^{\mathrm{T}}\hat{P}B_{\mathrm{f}}n(t)\\
&\leq -(\lambda_{\min}(RP^{-1}) - 1)\|P^{1/2}e_\xi(t)\|^2\\
&\quad - \lambda_{\min}(\tilde{R}\tilde{P}^{-1})\|\tilde{P}^{1/2}\tilde{\xi}(t)\|^2\\
&\quad - \Big(\lambda_{\min}(\hat{R}) - \|\hat{P}B_{\mathrm{f}}CP^{-1/2}\|\Big)\|\tilde{x}_{\mathrm{f}}(t)\|^2\\
&\quad - 2e_\xi^{\mathrm{T}}(t)(P + \tilde{P})B_0\tilde{W}_1^{\mathrm{T}}(t)\sigma_1(\zeta(t))\\
&\quad - 2e_\xi^{\mathrm{T}}(t)(P + \tilde{P})B_0\tilde{W}_2^{\mathrm{T}}(t)[I_m \otimes \sigma_2(\zeta(t))]u(t)\\
&\quad + 2e_\xi^{\mathrm{T}}(t)PB_0(\varepsilon_1(x(t)) + \varepsilon_2(x(t))u(t))\\
&\quad + 2e_\xi^{\mathrm{T}}(t)PB_0(W_1^{\mathrm{T}}[\hat{\sigma}_1(x(t)) - \sigma_1(\zeta(t))]\\
&\quad + W_2^{\mathrm{T}}\left[I_m \otimes (\hat{\sigma}_2(x(t)) - \sigma_2(\zeta(t)))\right]u(t))\\
&\quad - 2\tilde{\xi}^{\mathrm{T}}(t)\tilde{P}B_0(\varepsilon_1(x(t)) + \varepsilon_2(x(t))u(t))\\
&\quad - 2\tilde{\xi}^{\mathrm{T}}(t)\tilde{P}B_0(W_1^{\mathrm{T}}[\hat{\sigma}_1(x(t)) - \sigma_1(\zeta(t))]\\
&\quad + 2\|\tilde{x}_{\mathrm{f}}(t)\|\|\hat{P}B_{\mathrm{f}}\|n^*\\
&\quad + W_2^{\mathrm{T}}\left[I_m \otimes (\hat{\sigma}_2(x(t)) - \sigma_2(\zeta(t)))\right]u(t))\\
&\quad + 2(e_\xi^{\mathrm{T}}(t)P - \tilde{\xi}^{\mathrm{T}}(t)\tilde{P})B_0(\hat{W}_1(t) - \hat{W}_{1\mathrm{u}}(t))^{\mathrm{T}}\sigma_1(\zeta(t))\\
&\quad + 2\,\mathrm{tr}\,\tilde{W}_1^{\mathrm{T}}(t)\Big[\mathrm{Proj}(\hat{W}_1(t), -\sigma_1(\zeta(t))\xi_{\mathrm{c}}^{\mathrm{T}}(t)\tilde{P}B_0)\\
&\quad + \sigma_1(\zeta(t))\xi_{\mathrm{c}}^{\mathrm{T}}(t)\tilde{P}B_0\Big] + 2\,\mathrm{tr}\,\tilde{W}_2^{\mathrm{T}}(t)
\end{aligned}
$$

$$
\begin{aligned}
&\cdot \Big[\mathrm{Proj}(\hat{W}_2(t), -[I_m \otimes \sigma_2(\zeta(t))]u(t)\xi_{\mathrm{c}}^{\mathrm{T}}(t)\tilde{P}B_0) \\
&\quad + [I_m \otimes \sigma_2(\zeta(t))]u(t)\xi_{\mathrm{c}}^{\mathrm{T}}(t)\tilde{P}B_0\Big] \\
&\leq -(\lambda_{\min}(RP^{-1}) - 1)\|P^{1/2}e_\xi(t)\|^2 \\
&\quad - \lambda_{\min}(\tilde{R}\tilde{P}^{-1})\|\tilde{P}^{1/2}\tilde{\xi}(t)\|^2 \\
&\quad - \left(\lambda_{\min}(\hat{R}) - \|\hat{P}B_{\mathrm{f}}CP^{-1/2}\|\right)\|\tilde{x}_{\mathrm{f}}(t)\|^2 \\
&\quad - 2e_\xi^{\mathrm{T}}(t)(P + \tilde{P})B_0\tilde{W}_1^{\mathrm{T}}(t)\sigma_1(\zeta(t)) \\
&\quad - 2e_\xi^{\mathrm{T}}(t)(P + \tilde{P})B_0\tilde{W}_2^{\mathrm{T}}(t)[I_m \otimes \sigma_2(\zeta(t))]u(t) \\
&\quad + 2e_\xi^{\mathrm{T}}(t)PB_0(\varepsilon_1(x(t)) + \varepsilon_2(x(t))u(t)) \\
&\quad + 2e_\xi^{\mathrm{T}}(t)PB_0(W_1^{\mathrm{T}}[\hat{\sigma}_1(x(t)) - \sigma_1(\zeta(t))] \\
&\quad + W_2^{\mathrm{T}}\left[I_m \otimes (\hat{\sigma}_2(x(t)) - \sigma_2(\zeta(t)))\right]u(t)) \\
&\quad - 2\tilde{\xi}^{\mathrm{T}}(t)\tilde{P}B_0(\varepsilon_1(x(t)) + \varepsilon_2(x(t))u(t)) \\
&\quad - 2\tilde{\xi}^{\mathrm{T}}(t)\tilde{P}B_0(W_1^{\mathrm{T}}[\hat{\sigma}_1(x(t)) - \sigma_1(\zeta(t))] \\
&\quad + W_2^{\mathrm{T}}\left[I_m \otimes (\hat{\sigma}_2(x(t)) - \sigma_2(\zeta(t)))\right]u(t)) \\
&\quad + 2\|\tilde{x}_{\mathrm{f}}(t)\|\|\hat{P}B_{\mathrm{f}}\|n^* \\
&\quad + 2(e_\xi^{\mathrm{T}}(t)P - \tilde{\xi}^{\mathrm{T}}(t)\tilde{P})B_0(\hat{W}_1(t) - \hat{W}_{1\mathrm{u}}(t))^{\mathrm{T}}\sigma_1(\zeta(t)).
\end{aligned} \tag{55}
$$

For the two cases given in (48), the last term on the right-hand side of (55) gives

i) If $\hat{u}(t) \geq\geq 0$, $t \geq 0$, then $\hat{W}_{1\mathrm{u}}(t) = \hat{W}_1(t)$, and hence,

$$
2(e_\xi^{\mathrm{T}}(t)P - \tilde{\xi}^{\mathrm{T}}(t)\tilde{P})B_0(\hat{W}_1(t) - \hat{W}_{1\mathrm{u}}(t))^{\mathrm{T}}\sigma_1(\zeta(t)) = 0.
$$

ii) Otherwise, $\hat{W}_{1\mathrm{u}}(t) = 0$, and hence, for $t \geq 0$,

$$
\begin{aligned}
&2(e_\xi^{\mathrm{T}}(t)P - \tilde{\xi}^{\mathrm{T}}(t)\tilde{P})B_0(\hat{W}_1(t) - \hat{W}_{1\mathrm{u}}(t))^{\mathrm{T}}\sigma_1(\zeta(t)) \\
&\quad = 2(e_\xi^{\mathrm{T}}(t)P - \tilde{\xi}^{\mathrm{T}}(t)\tilde{P})B_0\hat{W}_1^{\mathrm{T}}(t)\sigma_1(\zeta(t)) \\
&\quad \leq 2\sqrt{s_1}\hat{w}_{1\max}\|P^{1/2}B_0\|\|P^{1/2}e_\xi(t)\| \\
&\qquad + 2\sqrt{s_1}\hat{w}_{1\max}\|\tilde{P}^{1/2}B_0\|\|\tilde{P}^{1/2}\tilde{\xi}(t)\|.
\end{aligned}
$$

Hence, it follows from (55) that in either case

$$
\begin{aligned}
&\dot{V}(e_\xi(t), e_z(t), \tilde{\xi}(t), \tilde{W}_1(t), \tilde{W}_2(t), \tilde{x}_{\mathrm{f}}(t)) \\
&\quad \leq -(\lambda_{\min}(RP^{-1}) - 1)\|P^{1/2}e_\xi(t)\|^2 \\
&\qquad - \lambda_{\min}(\tilde{R}\tilde{P}^{-1})\|\tilde{P}^{1/2}\tilde{\xi}(t)\|^2 \\
&\qquad - \left(\lambda_{\min}(\hat{R}) - \|\hat{P}B_{\mathrm{f}}CP^{-1/2}\|\right)\|\tilde{x}_{\mathrm{f}}(t)\|^2 \\
&\qquad + 2\sqrt{s_1}\hat{w}_{1\max}\|P^{-1/2}(P + \tilde{P})B_0\|\|P^{1/2}e_\xi(t)\| \\
&\qquad + 2\sqrt{ms_2}\hat{w}_{2\max}u^*\|P^{-1/2}(P + \tilde{P})B_0\|\|P^{1/2}e_\xi(t)\| \\
&\qquad + 2(\varepsilon_1^* + \varepsilon_2^*u^*)\|P^{1/2}B_0\|\|P^{1/2}e_\xi(t)\| \\
&\qquad + 2(\sqrt{s_1}\hat{w}_{1\max} + \sqrt{ms_2}\hat{w}_{2\max}u^*)\|P^{1/2}B_0\| \\
&\qquad \cdot \|P^{1/2}e_\xi(t)\| + 2(\sqrt{s_1}\hat{w}_{1\max} + \sqrt{ms_2}\hat{w}_{2\max}u^*) \\
&\qquad \cdot \|\tilde{P}^{1/2}B_0\|\|\tilde{P}^{1/2}\tilde{\xi}(t)\| \\
&\qquad + 2(\varepsilon_1^* + \varepsilon_2^*u^*)\|\tilde{P}^{1/2}B_0\|\|\tilde{P}^{1/2}\tilde{\xi}(t)\| \\
&\qquad + 2\sqrt{s_1}\hat{w}_{1\max}\|P^{1/2}B_0\|\|P^{1/2}e_\xi(t)\| \\
&\qquad + 2\sqrt{s_1}\hat{w}_{1\max}\|\tilde{P}^{1/2}B_0\|\|\tilde{P}^{1/2}\tilde{\xi}(t)\| \\
&\qquad + 2\|\tilde{x}_{\mathrm{f}}(t)\|\|\hat{P}B_{\mathrm{f}}\|n^* \\
&\quad = -(\lambda_{\min}(RP^{-1}) - 1)(\|P^{1/2}e_\xi(t)\| - \alpha_1)^2 + \nu \\
&\qquad - \lambda_{\min}(\tilde{R}\tilde{P}^{-1})(\|\tilde{P}^{1/2}\tilde{\xi}(t)\| - \alpha_2)^2 \\
&\qquad - \left(\lambda_{\min}(\hat{R}) - \|\hat{P}B_{\mathrm{f}}CP^{-1/2}\|\right)(\|\tilde{x}_{\mathrm{f}}(t)\| - \alpha_3)^2
\end{aligned} \tag{56}
$$

where ν, α_1, α_2, and α_3 are given by (34)–(37), respectively. Now, for

$$
\|P^{1/2}e_\xi\| \geq \alpha_{e_\xi} \triangleq \sqrt{\frac{\nu}{\lambda_{\min}(RP^{-1}) - 1}} + \alpha_1 \tag{57}
$$

or

$$
\|\tilde{P}^{1/2}\tilde{\xi}\| \geq \alpha_{\tilde{\xi}} \triangleq \sqrt{\frac{\nu}{\lambda_{\min}(\tilde{R}\tilde{P}^{-1})}} + \alpha_2 \tag{58}
$$

or

$$
\|\tilde{x}_{\mathrm{f}}\| \geq \alpha_{\tilde{x}_{\mathrm{f}}} \triangleq \sqrt{\frac{\nu}{\lambda_{\min}(\hat{R}) - \|\hat{P}B_{\mathrm{f}}CP^{-1/2}\|}} + \alpha_3 \tag{59}
$$

it follows that $\dot{V}(e_\xi(t), e_z(t), \tilde{\xi}(t), \tilde{W}_1(t), \tilde{W}_2(t), \tilde{x}_{\mathrm{f}}(t)) \leq 0$ for all $t \geq 0$, that is, $\dot{V}(e_\xi(t), e_z(t), \tilde{\xi}(t), \tilde{W}_1(t), \tilde{W}_2(t), \tilde{x}_{\mathrm{f}}(t)) \leq 0$ for all $(e_\xi(t), e_z(t), \tilde{\xi}(t), \tilde{W}_1(t), \tilde{W}_2(t), \tilde{x}_{\mathrm{f}}(t)) \in \tilde{\mathcal{D}}_e \backslash \tilde{\mathcal{D}}_{\mathrm{r}}$ and $t \geq 0$, where

$$
\begin{aligned}
\tilde{\mathcal{D}}_e \triangleq \Big\{&(e_\xi, e_z, \tilde{\xi}, \tilde{W}_1, \tilde{W}_2, \tilde{x}_{\mathrm{f}}) \in \mathbb{R}^m \times \mathbb{R}^{n-m} \times \mathbb{R}^r \\
&\times \mathbb{R}^{s_1 \times m} \times \mathbb{R}^{ms_2 \times m} \times \mathbb{R}^{n_{\mathrm{f}}} : x \in \mathcal{D}_{\mathrm{c}}\Big\}
\end{aligned} \tag{60}
$$

$$
\begin{aligned}
\tilde{\mathcal{D}}_{\mathrm{r}} \triangleq \Big\{&(e_\xi, e_z, \tilde{\xi}, \tilde{W}_1, \tilde{W}_2, \tilde{x}_{\mathrm{f}}) \in \mathbb{R}^m \times \mathbb{R}^{n-m} \times \mathbb{R}^r \\
&\times \mathbb{R}^{s_1 \times m} \times \mathbb{R}^{ms_2 \times m} \times \mathbb{R}^{n_{\mathrm{f}}} : \|P^{1/2}e_\xi\| \leq \alpha_{e_\xi}, \\
&\|\tilde{P}^{1/2}\tilde{\xi}\| \leq \alpha_{\tilde{\xi}}, \ \|x_{\mathrm{f}}\| \leq \alpha_{\tilde{x}_{\mathrm{f}}}\Big\}.
\end{aligned} \tag{61}
$$

Next, define

$$
\begin{aligned}
\tilde{\mathcal{D}}_\alpha \triangleq \Big\{&(e_\xi, e_z, \tilde{\xi}, \tilde{W}_1, \tilde{W}_2, \tilde{x}_{\mathrm{f}}) \in \mathbb{R}^m \times \mathbb{R}^{n-m} \times \mathbb{R}^r \times \mathbb{R}^{s_1 \times m} \\
&\times \mathbb{R}^{ms_2 \times m} \times \mathbb{R}^{n_{\mathrm{f}}} : V(e_\xi, e_z, \tilde{\xi}, \tilde{W}_1, \tilde{W}_2, \tilde{x}_{\mathrm{f}}) \leq \alpha\Big\}
\end{aligned} \tag{62}
$$

where α is the maximum value such that $\tilde{\mathcal{D}}_\alpha \subseteq \tilde{\mathcal{D}}_e$, and define

$$
\begin{aligned}
\tilde{\mathcal{D}}_\eta \triangleq \Big\{&(e_\xi, e_z, \tilde{\xi}, \tilde{W}_1, \tilde{W}_2, \tilde{x}_{\mathrm{f}}) \in \mathbb{R}^m \times \mathbb{R}^{n-m} \times \mathbb{R}^r \times \mathbb{R}^{s_1 \times m} \\
&\times \mathbb{R}^{ms_2 \times m} \times \mathbb{R}^{n_{\mathrm{f}}} : V(e_\xi, e_z, \tilde{\xi}, \tilde{W}_1, \tilde{W}_2, \tilde{x}_{\mathrm{f}}) \leq \eta\Big\}
\end{aligned} \tag{63}
$$

where

$$
\begin{aligned}
\eta > \beta(\mu) = \mu = \alpha_{e_\xi}^2 + \alpha_{\tilde{\xi}}^2 + \alpha_{\tilde{x}_{\mathrm{f}}}^2 + \lambda_{\max}(Q_1^{-1})\hat{w}_{1\max}^2 \\
+ \lambda_{\max}(Q_2^{-1})\hat{w}_{2\max}^2.
\end{aligned} \tag{64}
$$

To show ultimate boundedness of the closed-loop system (27), (28), and (49)–(51) assume[2] that $\tilde{\mathcal{D}}_\eta \subset \tilde{\mathcal{D}}_\alpha$. Now, since $\dot{V}(e_\xi, e_z, \tilde{\xi}, \tilde{W}_1, \tilde{W}_2, \tilde{x}_{\mathrm{f}}) \leq 0$ for all $(e_\xi, e_z, \tilde{\xi}, \tilde{W}_1, \tilde{W}_2, \tilde{x}_{\mathrm{f}}) \in \tilde{\mathcal{D}}_e \backslash \tilde{\mathcal{D}}_{\mathrm{r}}$ and $\tilde{\mathcal{D}}_{\mathrm{r}} \subset \tilde{\mathcal{D}}_\alpha$, it follows that $\tilde{\mathcal{D}}_\alpha$ is positively invariant. Hence, if $(e_\xi(0), e_z(0), \tilde{\xi}(0), \ \tilde{W}_1(0), \tilde{W}_2(0), \tilde{x}_{\mathrm{f}}(0)) \in \tilde{\mathcal{D}}_\alpha$, then it follows from Theorem 4.14 of [24] that the solution $(e_\xi(t), e_z(t), \tilde{\xi}(t), \ \hat{W}_1(t), \hat{W}_2(t))$, $t \geq 0$, to (27), (28), (49)–(51) is ultimately bounded with respect to $(e_\xi, \tilde{\xi}, \tilde{W}_1, \ \tilde{W}_2, \tilde{x}_{\mathrm{f}})$ uniformly in $e_z(0)$ with ultimate bound given by $\varepsilon = \alpha^{-1}(\eta) = \sqrt{\eta}$, which yields (33). In addition, since (50) is input-to-state stable with e_ξ viewed as the input, it follows from Proposition 4.4 of [24] that the solution $e_z(t)$, $t \geq 0$, to (50) is also ultimately bounded.

[2]This assumption ensures that in the error space $\tilde{\mathcal{D}}_e$ there exists at least one Lyapunov level set $\tilde{\mathcal{D}}_\eta \subset \tilde{\mathcal{D}}_\alpha$. Equivalently, imposing bounds on the adaptation gains ensures $\tilde{\mathcal{D}}_\eta \subset \tilde{\mathcal{D}}_\alpha$ [42]. In the case where the neural network approximation holds in $\mathbb{R}^n$ with delayed values, this assumption is automatically satisfied. See the discussion at the end of Theorem 3.1 for further details.

Next, it follows from Theorem 1 of [43] that there exist a continuously differentiable, radially unbounded, positive-definite function $V_z : \mathbb{R}^{n_z} \to \mathbb{R}$ and class $\mathcal{K}$ functions $\gamma_1(\cdot)$ and $\gamma_2(\cdot)$ such that

$$V_z'(e_z)\tilde{f}_z(e_\xi, e_z) \leq -\gamma_1(\|e_z\|), \quad \|e_z\| \geq \gamma_2(\|e_\xi\|). \tag{65}$$

Since the upper bound for $\|e_\xi\|^2$ is given by η, it follows that the set given by

$$\mathcal{D}_z \triangleq \left\{ z \in \mathbb{R}^{n-r} : V_z(z-z_e) \leq \max_{\|z-z_e\|=\gamma_2(\sqrt{\eta})} V_z(z-z_e) \right\} \tag{66}$$

is also positively invariant. Now, since $\tilde{\mathcal{D}}_\alpha$ and $\mathcal{D}_z$ are positively invariant, it follows that

$$\begin{aligned} \mathcal{D}_\alpha \triangleq \Big\{ & (x, \tilde{\xi}, \tilde{W}_1, \tilde{W}_2, \tilde{x}_{\mathrm{f}}) \in \mathbb{R}^n \times \mathbb{R}^r \times \mathbb{R}^{s_1 \times m} \times \mathbb{R}^{m s_2 \times m} \\ & \times \mathbb{R}^{n_{\mathrm{f}}} : V(\xi - y_{\mathrm{d}}, z - e_z, \tilde{\xi}, \hat{W}_1 - W_1, \hat{W}_2 - W_2, x_{\mathrm{f}} - x_{\mathrm{f}_e}) \\ & \leq \alpha \Big\} \end{aligned} \tag{67}$$

is also positively invariant. In addition, since (27), (28), (49)–(51), and (53) is ultimately bounded with respect to $(e_\xi, \tilde{\xi}, \tilde{W}_1, \tilde{W}_2, \tilde{x}_{\mathrm{f}})$ and (50) is input-to-state stable with e_ξ viewed as the input, it follows from Proposition 4.4 of [24] that the solution $(e_\xi(t), e_z(t), \tilde{\xi}(t), \tilde{W}_1(t), \tilde{W}_2(t), \tilde{x}_{\mathrm{f}}(t))$, $t \geq 0$, of the closed-loop system (27), (28), (49)–(51), and (53) is ultimately bounded for all $(e_\xi(0), e_z(0), \tilde{\xi}(0), \tilde{W}_1(0), \tilde{W}_2(0), \tilde{x}_{\mathrm{f}}(0)) \in \tilde{\mathcal{D}}_\alpha$.

Finally, $u(t) \geq\geq 0$, $t \geq 0$, is a restatement of (25). Now, since $G(x(t)) \geq\geq 0$, $t \geq 0$, and $u(t) \geq\geq 0$, $t \geq 0$, it follows from Proposition 2.1 that $x(t) \geq\geq 0$, $t \geq 0$, for all $x_0 \in \overline{\mathbb{R}}_+^n$. □

REFERENCES

[1] I. J. Rampil, "A primer for EEG signal processing in anesthesia," *Anesthesiology*, vol. 89, no. 4, pp. 980–1002, 1998.

[2] R. G. Bickford, "Automatic electroencephalographic control of general anesthesia," *Electroencephalographic Clin. Neurophysiol.*, vol. 2, pp. 93–96, 1950.

[3] J. W. Bellville and G. M. Attura, "Servo control of general anesthesia," *Science*, vol. 126, pp. 827–830, 1957.

[4] H. Schwilden and H. Stoeckel, "Quantitative EEG analysis during anesthesia with isoflurane in nitrous oxide at 1.3 and 1.5 MAC," *Brit. J. Anaesth.*, vol. 59, pp. 738–745, 1987.

[5] J. C. Scott, K. V. Ponganis, and D. R. Stanski, "EEG quantification of narcotic effect: The comparative pharmacodynamics of fentanyl and alfentanyl," *Anesthesiology*, vol. 62, pp. 234–241, 1985.

[6] A. Sidi, P. Halimi, and S. Cotev, "Estimating anesthetic depth by electroencephalography during anesthetic induction and intubation in patients undergoing cardiac surgery," *J. Clin. Anesth.*, vol. 2, pp. 101–107, 1990.

[7] P. S. Sebel, E. Lang, I. J. Rampil, P. F. White, R. Cork, M. Jopling, N. T. Smith, P. S. Glass, and P. Manberg, "A multicenter study of bispectral electroencephalogram analysis for monitoring anesthetic effect," *Anesth. Analg.*, vol. 84, no. 4, pp. 891–899, 1997.

[8] P. S. Glass, M. Bloom, L. Kearse, C. Roscow, P. Sebel, and P. Manberg, "Bispectral analysis measures sedation and memory effects of propofol, midazolam, isoflurane, and alfentanil in normal volunteers," *Anesthesiology*, vol. 86, pp. 836–847, 1997.

[9] G. Plourde, "BIS EEG monitoring: What it can and cannot do in regard to unintentional awareness," *Can. J. Anesth.*, vol. 49, p. R12, 2002.

[10] J. W. Johansen and P. S. Sebel, "Development and clinical application of electroencephalographic bispectrum monitoring," *Anesthesiology*, vol. 93, pp. 1336–1340, 2000.

[11] W. M. Haddad, T. Hayakawa, and J. M. Bailey, "Adaptive control for nonnegative and compartmental dynamical systems with applications to general anesthesia," *Int. J. Adapt. Control Signal Process.*, vol. 17, no. 3, pp. 209–235, 2003.

[12] W. M. Haddad, T. Hayakawa, and J. M. Bailey, "Adaptive control for nonlinear compartmental dynamical systems with applications to clinical pharmacology," *Syst. Control Lett.*, vol. 55, pp. 62–70, 2006.

[13] W. M. Haddad, J. M. Bailey, T. Hayakawa, and N. Hovakimyan, "Neural network adaptive output feedback control for intensive care unit sedation and intraoperative anesthesia," *IEEE Trans. Neural Netw.*, vol. 18, pp. 1049–1066, 2007.

[14] T. Hayakawa, W. M. Haddad, N. Hovakimyan, and J. M. Bailey, "Neural network adaptive dynamic output feedback control for nonlinear nonnegative systems using tapped delay memory units," in *Proc. Amer. Control Conf.*, Boston, MA, Jun. 2004, pp. 3409–3414.

[15] J. M. Bailey, W. M. Haddad, J. J. Im, and T. Hayakawa, "Adaptive and neural network adaptive control of depth of anesthesia during surgery," in *Proc. Amer. Control Conf.*, Minneapolis, MN, Jun. 2006, pp. 3409–3414.

[16] A. Berman and R. J. Plemmons, *Nonnegative Matrices in the Mathematical Sciences*. New York: Academic Press, 1979.

[17] W. M. Haddad and V. Chellaboina, "Stability and dissipativity theory for nonnegative dynamical systems: A unified analysis framework for biological and physiological systems," *Nonlinear Anal.: Real World Appl.*, vol. 6, pp. 35–65, 2005.

[18] C. I. Byrnes and A. Isidori, "Asymptotic stabilization of minimum phase nonlinear systems," *IEEE Trans. Autom. Control*, vol. 36, no. 10, pp. 1122–1137, Oct. 1991.

[19] A. Isidori, *Nonlinear Control Systems*. New York: Springer, 1995.

[20] C.-T. Chen, *Linear System Theory and Design*. New York: Holt, Rinehart, and Winston, 1984.

[21] H. L. Royden, *Real Analysis*. New York: Macmillan, 1988.

[22] F. L. Lewis, S. Jagannathan, and A. Yesildirak, *Neural Network Control of Robot Manipulators and Nonlinear Systems*. London, U.K.: Taylor & Francis, 1999.

[23] E. Lavretsky, N. Hovakimyan, and A. J. Calise, "Upper bounds for approximation of continuous-time dynamics using delayed outputs and feedforward neural networks," *IEEE Trans. Autom. Control*, vol. 48, no. 9, pp. 1606–1610, Sep. 2003.

[24] W. M. Haddad and V. Chellaboina, *Nonlinear Dynamical Systems and Control: A Lyapunov-Based Approach*. Princeton, NJ: Princeton Univ. Press, 2008.

[25] P. De Leenheer and D. Aeyels, "Stabilization of positive linear systems," *Syst. Control Lett.*, vol. 44, no. 4, pp. 259–271, 2001.

[26] P. De Leenheer and D. Aeyels, "Stability properties of classes of cooperative systems," *IEEE Trans. Autom. Control*, vol. 46, no. 12, pp. 1996–2001, Dec. 2001.

[27] B. Marsh, M. White, N. Morton, and G. N. Kenny, "Pharmacokinetic model driven infusion of propofol in children," *Brit. J. Anaesth.*, vol. 67, no. 1, pp. 41–48, 1991.

[28] R. N. Upton, G. I. Ludrook, C. Grant, and A. Martinez, "Cardiac output is a determinant of the initial concentration of propofol after short-term administration," *Anesth. Analg.*, vol. 89, no. 3, pp. 545–552, 1999.

[29] M. Muzi, R. A. Berens, J. P. Kampine, and T. J. Ebert, "Venodilation contributes to propofol-mediated hypotension in humans," *Anesth. Analg.*, vol. 74, no. 6, pp. 877–883, 1992.

[30] E. F. Ismail, S. J. Kim, and M. R. Salem, "Direct effects of propofol on myocardial contractility in situ canine hearts," *Anesthesiology*, vol. 79, no. 5, pp. 964–972, 1992.

[31] A. V. Hill, "The possible effects of the aggregation of the molecules of hemoglobin on its dissociation curve," *J. Physiol.*, vol. 40, pp. iv–vii, 1910.

[32] T. Kazama, K. Ikeda, K. Moritu, M. Kikura, M. Doi, T. Ikeda, and T. Kurita, "Comparison of the effect site Ke0s of propofol for blood pressure and EEG bispectral index in elderly and young patients," *Anesthesiology*, vol. 90, pp. 1517–1527, 1999.

[33] R. G. Eckenhoff and J. S. Johansson, "On the relevance of "clinically relevant concentrations" of inhaled anesthetics in in vitro experiments," *Anesthesiology*, vol. 91, no. 3, pp. 856–860, 1999.

[34] J. C. Sigl and N. G. Chamoun, "An introduction to bispectral analysis for the electroencephalogram," *Anesthesiology*, vol. 10, no. 6, pp. 392–404, 1994.

[35] E. Mortier, M. Struys, T. De Smet, L. Versichelen, and G. Rolly, "Closed-loop controlled administration of propofol using bispectral analysis," *Anaesthesia*, vol. 53, no. 8, pp. 749–754, 1998.

[36] T. W. Schnider, C. F. Minto, and D. R. Stanski, "The effect compartment concept in pharmacodynamic modelling," *Anaes. Pharmacol. Rev.*, vol. 2, pp. 204–213, 1994.
[37] J. A. Jacquez and C. P. Simon, "Qualitative theory of compartmental systems," *SIAM Rev.*, vol. 35, pp. 43–79, 1993.
[38] H. Schwilden, J. Schutler, and H. Stoeckel, "Closed-loop feedback control of methohexital anesthesia by quantitative EEG analysis in humans," *Anesthesiology*, vol. 67, pp. 341–347, 1987.
[39] M. Struys, T. De Smet, L. Versichelen, S. Van de Velde, R. Van den Broecke, and E. Mortier, "Comparison of closed-loop controlled administration of propofol using BIS as the controlled variable versus "standard practice" controlled administration," *Anesthesiology*, vol. 95, pp. 6–17, 2001.
[40] X.-S. Zhang, R. J. Roy, and E. W. Jensen, "EEG complexity as a measure of depth of anesthesia for patients," *IEEE Trans. Biomed. Eng.*, vol. 48, no. 12, pp. 1424–1433, Dec. 2001.
[41] P. S. Glass and I. J. Rampil, "Automated anesthesia: fact or fantasy?," *Anesthesiology*, vol. 95, no. 12, pp. 1–2, 2001.
[42] N. Hovakimyan, F. Nardi, A. Calise, and N. Kim, "Adaptive output feedback control of uncertain nonlinear systems using single-hidden-layer neural networks," *IEEE Trans. Neural Netw.*, vol. 13, no. 6, pp. 1420–1431, Nov. 2002.
[43] E. D. Sontag and Y. Wang, "On characterizations of the input-to-state stability property," *Syst. Control Lett.*, vol. 24, no. 12, pp. 351–359, 1995.

Wassim M. Haddad (S'87–M'87–SM'01–F'09) received the B.S., M.S., and Ph.D. degrees in mechanical engineering from Florida Institute of Technology, Melbourne, in 1983, 1984, and 1987, respectively, with specialization in dynamical systems and control.

From 1987 to 1994, he served as a consultant for the Structural Controls Group of the Government Aerospace Systems Division, Harris Corporation, Melbourne, FL. In 1988, he joined the faculty of the Mechanical and Aerospace Engineering Department at Florida Institute of Technology, where he founded and developed the Systems and Control Option within the graduate program. Since 1994, he has been a member of the faculty in the School of Aerospace Engineering, Georgia Institute of Technology, Atlanta, where he holds the rank of Professor. His research contributions in linear and nonlinear dynamical systems and control are documented in over 500 archival journal and conference publications. He is a coauthor of the books *Hierarchical Nonlinear Switching Control Design with Applications to Propulsion Systems* (Springer-Verlag, 2000), *Thermodynamics: A Dynamical Systems Approach* (Princeton University Press, 2005), *Impulsive and Hybrid Dynamical Systems: Stability, Dissipativity, and Control* (Princeton University Press, 2006), *Nonlinear Dynamical Systems and Control: A Lyapunov-Based Approach* (Princeton University Press, 2008), and *Nonnegative and Compartmental Dynamical Systems* (Princeton University Press, 2010). His recent research is concentrated on nonlinear robust and adaptive control, nonlinear dynamical system theory, large-scale systems, hierarchical nonlinear switching control, analysis and control of nonlinear impulsive and hybrid systems, adaptive and neuroadaptive control, system thermodynamics, thermodynamic modeling of mechanical and aerospace systems, network systems, expert systems, nonlinear analysis and control for biological and physiological systems, and active control for clinical pharmacology.

Dr. Haddad is an NSF Presidential Faculty Fellow and a member of the Academy of Nonlinear Sciences.

Kostyantyn Y. Volyanskyy (S'07) received the B.S., M.S., and Ph.D. degrees in applied mathematics from National Taras Shevchenko University of Kyiv, Kiev, Ukraine, in 1998, 1999, and 2003, respectively, with specialization in modeling and control of complex dynamical systems. He is currently pursuing the Ph.D. degree in aerospace engineering from the School of Aerospace Engineering, Georgia Institute of Technology, Atlanta.

Since 2004, he has been with the School of Aerospace Engineering, Georgia Institute of Technology. His research interests include nonlinear adaptive control and estimation, neural networks and intelligent control, nonlinear analysis and control for biological and physiological systems, and active control for clinical pharmacology.

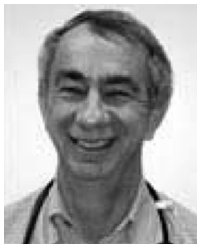

James M. Bailey received the B.S. degree from Davidson College, Davidson, NC, in 1969, the Ph.D. degree in chemistry (physical) from the University of North Carolina at Chapel Hill, Chapel Hill, in 1973, and the M.D. degree from Southern Illinois University School of Medicine, Springfield, IL, in 1982.

He was a Helen Hay Whitney Fellow with the California Institute of Technology from 1973–1975 and Assistant Professor of chemistry and biochemistry at Southern Illinois University from 1975–1979. After receiving his M.D. degree, he completed a residency in anesthesiology and then a fellowship in cardiac anesthesiology at the Emory University School of Medicine affiliated hospitals. From 1986–2002 he was an Assistant Professor of anesthesiology and then Associate Professor of anesthesiology at Emory, where he also served as director of the critical care service. In September 2002, he moved his clinical practice to Northeast Georgia Medical Center, Gainesville, GA, as Director of Cardiac Anesthesia and Consultant in critical care medicine. He has served as Chief Medical Officer of Northeast Georgia Health Systems since 2008. He is board certified in anesthesiology, critical care medicine, and transesophageal echocardiography. His research interests have focused on pharmacokinetic and pharmacodynamic modeling of anesthetic and vasoactive drugs and, more recently, applications of dynamical system theory in medicine. He is the author or coauthor of 100 journal articles, conference publications, or book chapters.

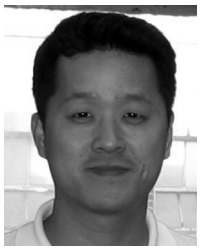

Jeong Joon Im (S'06) received the B.S. degree in mechanical engineering from the Hanyang University, Seoul, South Korea, in 1993, the M.Eng. degree in mechanical engineering from Korea University, Seoul, South Korea, in 1997, and the M.S. degree in aerospace engineering from the Georgia Institute of Technology, Atlanta, in 2008. He is currently pursuing the Ph.D. degree in mechanical engineering from the Department of Mechanical Engineering, Virginia Polytechnic Institute and State University, Blacksburg.

In 2008, he joined the Department of Mechanical Engineering, Virginia Polytechnic Institute and State University. His research interests include analysis and control of biomedical systems, adaptive control, unmanned aerial vehicles, experiment design and organization, and hardware/software interface.